A Dual Toll Policy for Regulating the Transportation of Hazardous Materials

by

Huiwen Zhang

A thesis
presented to the University of Waterloo
in fulfillment of the
thesis requirement for the degree of
Master of Applied Science
in
Management Sciences

Waterloo, Ontario, Canada, 2018

I hereby declare that I am the sole author of this thesis. This is a true copy of the thesis, including any required final revisions, as accepted by my examiners.

I understand that my thesis may be made electronically available to the public.

Abstract

The transportation of hazardous materials (hazmat) has drawn significant attention from various stakeholders due to the undesirable impacts on the environment and public health. Focusing on the connection between the traffic and the risk associated with the hazmat shipments, the present research aims to assist the regulator in designing a policy of dual tolls, imposed on both hazmat and non-hazmat shipments, to mitigate the hazmat risk in a road network.

A bi-objective bi-level programming formulation is constructed. To be specific, the upper level model indicates the regulator's decision problem, minimizing the maximum link risk and the total network risk by imposing a dual-toll policy on any carrier. The lower level jointly considers the decisions of multiple hazmat carriers and non-hazmat travelers, minimizing the total transportation cost, including the toll cost. (By "non-hazmat traveler", we mean both people who carry and do not carry products.)

Given the bi-level structure and the non-linear nature, a solution procedure with two parts is designed. First, we develop two alternative linearization approaches. One is piecewise linearization, transforming the non-linear terms into linear ones. The other applies the Frank-Wolfe algorithm, an iterative first-order optimization algorithm. Then a genetic-algorithm-based methodology will integrate both levels. Computational experiments on different sizes of networks are performed to demonstrate the effectiveness of the model. Various analyses, involving trade-offs, sensitivities, and examination of convergence, are conducted to provide additional managerial insights. These can be used to facilitate stakeholders' decision making.

Acknowledgements

First, I want to convey my utmost gratitude to my supervisors, Professors James Bookbinder and Ginger Y. Ke, for their guidance and support of my research. It is a valuable experience for me to learn from you. Thanks also go to my reading committee, Professors Sibel Alumur Alev and Joe Naoum-Sawaya, for their insightful opinions.

Second, I would like to thank my parents for their endless love and continuous support. Especially, my common-law partner, Xin Sui, thank you for encouraging me all the time.

My gratitude extends to the faculty and staff of the Department of Management Sciences at the University of Waterloo.

Table of Contents

List of Tables

List of Figures

Chapter 1

Introduction

The United States Department of Transportation [US DOT, 2012] defines a hazardous material (hazmat) to be any substance or material that is capable of causing harm to people, property and environment. Hazardous materials play important roles in industrialized societies.The United Nations [UN, 2001] sorts hazardous materials into nine categories: "flammable and combustible liquids; flammable, combustible, and dangerous-when-wet solids; oxidizers and organic peroxides; poisonous and infectious materials; radioactive materials; corrosive materials (acidic or basic); and miscellaneous dangerous goods, such as hazardous wastes." In 2012, more than 98 percent of hazmat transportation was carried by a single mode, including road, rail, water, air and pipeline [US DOT, 2012]. Trucks account for nearly 70 percent of total single-mode hazmat shipments, due to the flexibility of this transportation mode.

Although the number of hazmat transportation accidents is fairly small compared with non-hazmat transportation, the consequences of hazmat transportation incidents, such as fatalities, injuries, accidents and property damage, can be catastrophic. In 2003, hazmat shipments triggered only 3.2 percent of all traffic incidents; however, those led to

15 deaths, 117 injuries and $ 48.6 million of property loss [US DOT, 2004a].

On July 1, 2009, a fiery crash between a car and a tanker truck in Southern New Jersey caused the release of 13 gallons of gasoline and the death of the car driver. The property damage was about $ 27,000, and Route 40 had to be closed for nearly 8 hours [National Transportation Safety Board, 2009]. On July 6, 2013, a 74-car freight train carrying crude oil derailed in Lac-Mégantic, Quebec, Canada, causing the explosion of multiple tanks. This disaster resulted in 47 deaths, and nearly half of the town's area was destroyed [National Post, 2013].

Multiple parties, for example, the government, carriers and shippers are involved in hazmat transportation. In each move of hazmats from origin to destination, different players have distinct priorities. From the government's perspective, the potential impacts of hazmat transportation on both population and environment necessitate effective and efficient ways to mitigate the associated risks. So, many governments have developed explicit regulations for hazmat transportation. These include the Federal Hazardous Materials Transportation Act in the United States, and the Federal Transportation of Dangerous Goods Act in Canada.

Despite the concerns about hazmat risks, governments at various levels may each have an individual focus. More specifically, the local government may want to ensure equity on the spatial distribution of risk, whereas the regional government may pay more attention to the total network risk [Bianco et al., 2013]. However, for transportation carriers, i.e., trucking companies, the major concern is cost. In other words, a carrier is more interested in finding routes with minimum transportation cost. Some paths are shorter but require travel through densely populated zones; other paths may avoid the populated area but have higher cost. Finally, some paths have minimum travel time with the use of highways, but may lead to a greater accident rate. Hence, the hazmat

transportation problem is a multiobjective problem with several players [Erkut et al., 2007].

Normally, the government does not have the right to choose specific routes for hazmat carriers. What they can do, however, is regulate the use of roads for hazmat carriers through certain policies. Two types of policies are widely used nowadays. One is based upon the Hazmat Transportation Network Design (HTND) Problem, and the other is referred to as the Toll Setting (TS) policy. In the hazmat network design problem, the authority closes certain segments of roads for hazmat carriers or sets an upper limit of hazmat flow on certain links of such roads. A detailed review of this policy can be found in Section 2.4.

Unlike the HTND problem, which puts certain restrictions on links of the network, a toll setting policy imposes toll costs on particular links, so as to transfer more shipments to less-populated links. Compared with the hazmat network design problem, carriers have more flexibilities to respond to a toll setting policy. They are more willing to choose less-risky routes based on their own decisions to reduce the total transportation cost. Recently, a novel policy called $dual\ toll\ pricing$ was proposed by Wang et al. [2012]. As opposed to the single toll setting, this policy takes regular traffic into consideration, in addition to hazmat, because the congestion posed by traffic overall may increase the probability of an incident.

It is clear that the main concern of a government authority is to control the risk induced by hazmat transportation on the population and the environment. Apart from the minimization of total risk, the authority should also promote $equity$ in the spatial distribution of risk. This becomes crucial when certain populated zones are exposed to an intolerable level of risk, resulting from the carriers' routing decisions. Properly defined by Keeney [1980], risk equity diminishes the largest differences of risks among

people. When applying hazmat transportation network design or a toll setting policy, most researchers focus only on total risk, yet neglect the risk equity. Ignoring the latter may cause more hazmat shipments in one specific area than in others, which leads to a greater probability of exposure for the residents of the former area.This lack of equity is one major reason that, recently, more and more people oppose hazmat transportation. Realizing the impact of risk equity, in this thesis we investigate the tradeoff between total risk and risk equity.

To address traffic congestion, this research proposes a dual toll policy, which can be applied to both hazmat and non-hazmat shipments, to mitigate the risk associated with the hazmat transportation. The contribution of this work is fourfold. Firstly, a bi-level bi-objective non-linear programming model for hazmat transportation is developed and tested. Specifically, in the upper level, the total risks and the risk equity are minimized from the points of view of the regional and local governments, respectively. Then in the lower level, the transportation costs for both regular travellers and hazmat carriers are considered. To the best of our knowledge, the majority of previous research considers only the relationships between a single level of government and one hazmat carrier.

Secondly, to more practically reflect the real-world situations, several carriers that transport multiple hazmats are considered in our proposed model. As far as we know, very few papers in the literature include multiple hazmats in their research. Thirdly, we develop a genetic-algorithm-based solution procedure, integrated with a piecewise linearization process or the Frank-Wolfe algorithm, to solve the mathematical model with a satisfactory solution in a reasonable computational time. Finally, several numerical instances with different network sizes are used to demonstrate the effectiveness of our model. Various analyses, such as trade-off analysis, sensitivity analysis, and convergence examination, are conducted to provide additional managerial insights, which can be

used to facilitate decision making of the various stakeholders.

The remainder of this thesis is organized as follows. A literature review emphasising hazmat transportation and bi-level models is provided in Chapter 2. In Chapter 3, we propose our mathematical formulation for hazmat transporation that also considers the regular traffic. Based on the model of Chapter 3, the solution procedure including linearization, the Frank-Wolfe algorithm and a GA-based algorithm is outlined in Chapter 4. Moreover, several numerical experiments are conducted and discussed in Chapter 5. Chapter 6 concludes the thesis and suggests future research directions.

Chapter 2

Literature review

This chapter reviews several streams of research relevant to the present study: 1) risk assessment in hazmat transportation, 2) risk equity consideration, 3) bi-level programming models, 4) the applications of bi-level models in hazmat transportation and 5) dual toll pricing.

2.1 Risk Assessment

The risk of an accident during the transport of hazardous materials makes the hazmat transportation problem much more complicated than when non-hazardous goods are moved. Therefore, great effort has been made to capture the risk in hazmat transportation. Below are several risk evaluation models that are useful for this purpose.

Traditional Risk (TR) model The U.S. Department of Transportation (1989) defined risk as the product of the probability and the consequence of an incident. Normally, the

consequence can be quantified as the size of the affected population within a certain distance of the incident site; the probability of the incident is associated with the nature of substances shipped and the road type. Abkowitz and Cheng [1988] argued that the incident probability is usually between 10^{-8} and 10^{-6} per mile travelled. To be specific,

$$TR(P) = \sum_{(i,j)\in P} p_{ij} C_{ij}, \tag{2.1}$$

where P is the path which contains arcs from node i to node j. p_{ij} and C_{ij} are the probability and the consequence for specific arc (i, j). The definitions of p_{ij} and C_{ij} will apply to all the models in this section.

Incident Probability (IP) model When we assume that the variance in population density can be ignored, the TR model can be simplified to the IP model. First introduced by Saccomanno and Chan [1985], the IP model is appropriate for hazmats whose impact on the surrounding population is relatively small. For this model, the risk is evaluated as

$$IP(P) = \sum_{(i,j)\in P} p_{ij}. \tag{2.2}$$

Note the difference between this equation and Eq. (2.1).

Population Exposure (PE) model The Population Exposure model was first proposed by Batta and Chiu [1988], and then used by ReVelle et al. [1991] in a study commissioned by the U.S. Department of Energy. This model considers only the consequence, i.e., the exposed population within the area surrounding an incident. The corresponding equation for risk is then:

$$PE(P) = \sum_{(i,j)\in P} C_{ij}. \tag{2.3}$$

Perceived Risk (PR) model Some researchers feel that the traditional risk model is not appropriate because it assumes a risk-neutral attitude. However, the majority of people have risk-averse attitudes toward hazmat transportation. This is because the consequence of any hazmat-related accident can be high, despite the low probability. Inspired by Saccomanno and Chan [1985], Abkowitz and Cheng [1988] suggested the perceived risk (PR) model by adding a new element, the exponent q, to the traditional risk model:

$$PR(P) = \sum_{(i,j)\in P} p_{ij}(C_{ij})^q. \tag{2.4}$$

When $q > 1$, this model represents a risk-averse attitude, while when $q = 1$, the model reduces to the traditional risk model, Eq. (2.1).

Conditional Risk (CR) model Another disadvantage of the Traditional Risk model is that it may not be accurate when multiple hazmat shipments occur on a specific path. An underlying assumption of the TR model is that a path can be used as many times as needed. However, if a catastrophic accident results in the exposure of certain hazardous materials on a specific path, then other carriers should reevaluate their use of that path. Sivakumar et al. (1993a, b; 1995) proposed a new model, called the Conditional Risk model, to apply to such a situation.

$$CR(P) = \frac{\sum_{(i,j)\in P} p_{ij}C_{ij}}{\sum_{(i,j)\in P} p_{ij}}. \tag{2.5}$$

Unlike the first four models, the CR model is a two-attribute model. The first attribute is traditional risk, and the second is incident probability.

Minimax Risk (MM) and Mean-Variance (MV) models The Minimax Risk model and the Mean-Variance model were introduced by Erkut and Ingolfsson [2000] as risk-averse models to lessen the likelihood of the catastrophic consequences of hazmat transportation. In the MM model, those authors minimized the maximum population exposure in the event of an incident. In the MV model, the variance of the consequence of each path is incorporated into the solution.

$$MM(P) = \max_{i,j \in P} C_{ij}, \tag{2.6}$$

$$MV(P) = \sum_{(i,j) \in P} (p_{ij} C_{ij} + k p_{ij} (C_{ij})^2), \tag{2.7}$$

where the number k is a given constant.

Disutility (DU) model Apart from the MM and MV models, Erkut and Ingolfsson [2000] also proposed a Disutility model which used explicit utility theory to reflect a risk-averse attitude toward hazmat transportation.

$$DU(P) = \sum_{(i,j) \in P} p_{ij} (\exp(k C_{ij} - 1)) \tag{2.8}$$

where k, a measure of the aversion to catastrophe, is a positive constant. Higher values of k represent greater degrees of risk.

A summary of the preceding popular risk measurements is shown in Table 2.1. The model proposed in our research is based on the PE model, which concerns the worst

case scenario of an incident. Moreover, we take the traffic congestion into consideration. Travel time is an important factor in measuring risk: the longer the travel time, the greater the risk. Hence, we integrate travel time with population in the PE model, to calculate risk at the specific site of an incident. A detailed explanation can be found in Section 3.1.

Table 2.1: Traditional Path Risk Evaluation Models (Adapted from Erkut and Ingolfsson, 2005)

Approach	Model	Sample reference
Traditional Risk	$TR(P) = \sum_{(i,j)\in P} p_{ij}C_{ij}$	Alp [1995]
Incident Probability	$IP(P) = \sum_{(i,j)\in P} p_{ij}$	Saccomanno and Chan [1985]
Population Exposure	$PE(P) = \sum_{(i,j)\in P} C_{ij}$	Batta and Chiu [1988], ReVelle et al. [1991]
Perceived Risk	$PR(P) = \sum_{(i,j)\in P} p_{ij}(C_{ij})^q$	Abkowitz and Cheng [1988]
Conditional Risk	$CR(P) = \frac{\sum_{(i,j)\in P} p_{ij}(C_{ij})^q}{\sum_{(i,j)\in P} p_{ij}}$	Sivakumar et al. [1993a, b; 1995]
Maximum Risk	$MM(P) = \max_{i,j\in P} C_{ij}$	Erkut and Ingolfsson [2000]
Mean-Variance	$MV(P) = \sum_{(i,j)\in P}(p_{ij}C_{ij} + kp_{ij}(C_{ij})^2)$	Erkut and Ingolfsson [2000]
Disutility	$DU(P) = \sum_{(i,j)\in P} p_{ij}(exp(kC_{ij} - 1))$	Erkut and Ingolfsson [2000]

2.2 Risk Equity Consideration

The primary concern of the government is to control the risk triggered by hazmat shipments over the surrounding area. Apart from the total network risk, the risk equity, i.e., the spatial distribution of risk, should also be considered. Defined by Keeney [1980], risk equity assesses and prunes the differences in the level of risk among a set of individuals [Carotenuto et al., 2007a]. As noted earlier, the consideration of risk equity is crucial because the hazmat carrier's routing or a scheduling decision may cause certain

population zones to be exposed to intolerable levels of risk [Erkut et al., 2007].

The issue of risk equity in hazmat transportation has been examined through different approaches. One method is to limit the risk associated with a population zone or a link. Gopalan et al. [1990] proposed an integer programming formulation to discover several ideal routes that not only minimize the total risk, but also spread that risk equitably over the region. To ensure risk equity, they partitioned the population area into different zones, and limited the difference of risks between any two zones. Threshold constraints, with bounded maximum risk on any link, were used to attain this. Carotenuto et al. [2007a] also bounded each link in the embedded network with a threshold to guarantee the equitable spreading of risk. Fang et al. [2017] introduced a mixed-integer programming model to route and schedule hazmat shipments by rail when there were due dates. Risk was expressed as an increasing function of speed. Limited by the risk threshold on each service leg, the speed-dependent risk was ensured to be spread equitably in the railway network.

Another approach that has been applied in the literature on risk equity is the minmax method. Current and Ratick [1995] formulated a mixed-integer program to locate facilities to handle hazmats. In their paper, risk equity was ensured by minimizing the maximum hazmat amounts respectively shipped past any individual person and any facility. Since it is a multiobjective model, they used the weighting method for its solution. Bell [2006] used the same minmax method to determine the safest set of routes, in the case of a risk-averse attitude towards hazmat shipments.

Finding dissimilar paths is also regarded as an approach to guarantee the risk equity [Carotenuto et al., 2007a]. Akgün et al. [2000] introduced two methods, the Iterative Penalty Method (IPM) and the Gateway Shortest Paths (GSPs), to find dissimilar paths. Based on the repetitive application on the shortest path algorithm, IPM imposes a different

penalty coefficient on each selected link to prevent drivers from choosing the same path; GSPs require that carriers go through specific nodes, called “gateways". However, finding dissimilar paths cannot always be used to ensure risk equity. For example, if two selected dissimilar paths have only a few links in common, but are very close to each other in geography, then people living around the intersection of the exposure zones face greater risks.

Kang et al. [2014] integrated the Value-at-Risk (VaR) framework in a model for the routing of multiple hazmat types. The route was chosen based on the global VaR calculation, and risk equity was met by setting a specific threshold for each zone. Romero et al. [2016] developed a novel model, which applied the Gini coefficient, an index first used to express the inequality in the wealth distribution of a nation’s residents. The Gini-coefficient-based model seeks to attain risk equity in analysing hazmat facility locations and routing decisions. With a given set of minimum risk routes and departure times, Carotenuto et al. [2007b] proposed a model to minimize the total shipment delay, while ensuring the risk equity. In that model, to achieve the latter goal, the authors discouraged carriers from travelling too close to each other.

Despite the criticality of maintaining an equitable distribution of risk, risk equity is a major concern for the government, but not the carrier. Therefore, it is usually the government authority that poses the equity restrictions. The dominant power of the authority over the carrier, and the interactions between the decisions of these two parties, suggest the use of a bi-level programming model. That can actually reflect this leader-follower situation. Details about the bi-level model and its application in the hazmat transportation area (including the consideration of risk equity) are reviewed in the following sections.

2.3 Bi-level Programming Model

Rooted in the Stackelberg game [Von Stackelberg, 1934], a bi-level model can be used to formulate the non-cooperative decision process of two decision makers. The leader (upper level), the decision maker with the dominant power, is constrained by the behavior of the follower, while the follower (lower level) can only find the best solution under the feasible region defined by the leader. The general formulation of a bi-level programming problem is:

$$\min F(x, y), \tag{2.9}$$

Subject to:

$$G(x, y) \leq 0, \tag{2.10}$$

$$x \in R^{n_1}, \tag{2.11}$$

$$\arg\min_{y} f(x, y), \tag{2.12}$$

Subject to:

$$g(x, y) \leq 0 \tag{2.13}$$

$$y \in R^{n_2}. \tag{2.14}$$

The variables of the above problem are classified as the upper level variables $x \in R^{n_1}$ and the lower level variables $y \in R^{n_2}$. $F : R^{n_1} \times R^{n_2} \to R$ and $f : R^{n_1} \times R^{n_2} \to R$ are the upper-level and lower-level objective functions, respectively. The vector-valued functions $G : R^{n_1} \times R^{n_2} \to R^{m_1}$ and $g : R^{n_1} \times R^{n_2} \to R^{m_2}$ are respectively called the upper-level and lower-level constraints. R^{n_1} is the feasible region of the upper level problem, and R^{n_2} is

the feasible region of the lower level problem, given the upper level variables which have already been worked out.

A bi-level model, even in a linear format, is hard to solve. Hansen et al. [1992] and Vicente et al. [1996] have proved linear bi-level programs to be strongly NP-hard. Up to now, several solution methods, such as extreme point approaches [Candler and Townsley, 1982], complementary pivoting [Bialas et al., 1980], KKT-based approaches [Kara and Verter, 2004; Bianco et al., 2013], and duality-based methods [Marcotte et al., 2009], have been developed to deal with linear bi-level models. Nevertheless, all these approaches are not likely to work in our case, given the non-linear nature of our lower-level model.

Apart from the above methods, in the recent 20 years, a variety of metaheuristic techniques have been proposed to solve bi-level models. Compared with other techniques, the major strength of metaheuristics is that it can be applied to a model of any form. For example, branch-and-bound and complementary pivoting can just solve *linear* bi-level models. That is because only when the lower level is convex and regular, can Karush-Kuhn-Tucker (KKT) conditions be applied to the lower level, and transform the bi-level to a single-level model. Metaheuristics have no such limitations, and therefore are a better choice for large and complex models.

Unlike exact methods, metaheuristics deal with problems by generating satisfactory solutions in a reasonable time. Marinakis and Marinaki [2013] introduced a particle swarm optimization algorithm for solving two supply chain management problems: vehicle routing and location-routing problems. A tabu-search-based metaheuristic, proposed by Aksen and Aras [2013], was used to deal with a facility location protection-interdiction bi-level model. Arroyo and Fernández [2013] applied a genetic algorithm to analyse the vulnerability of power systems under multiple contingencies.

In our research, a genetic-algorithm-based solution procedure is developed to search

for the optimal solution to our bi-objective bi-level programming model. Details regarding this procedure are discussed in Chapter 4.

2.4 Bi-level Model Applications In Hazmat Transportation

In this section, we focus our review on the two most popular applications of bi-level models in hazmat transportation, namely the network design (HTND) and toll setting (TS) policies.

2.4.1 Hazmat Transportation Network Design (HTND)

Normally, the government does not have the authority to impose specific routes on hazmat carriers. But it is possible for the government to close certain segments of roads near highly-populated areas, so that the impact on the environment can be reduced. This approach is called the network design policy.

Kara and Verter [2004] were the first to provide a bi-level programming formulation for the hazmat transportation network design problem. Their approach differed from previous papers because of its emphasis on the relationship between the government and carriers in designing a road network for hazmat transportation. In the bi-level model, the government chose the road segments to be closed to minimize the total risk, while the carriers selected the path from the 'new' network based on minimum cost. Kara and Verter [2004] transformed the bi-level program into a single-level mixed integer program by replacing the lower level problem with its KKT conditions. Erkut and Gzara [2008] generalized the model of Kara and Verter [2004] to the undirected case. Transport cost was

added to analyse possible tradeoffs between risk and cost. This was the first bi-objective, bi-level model in the network design literature. Bianco et al. [2009] introduced a linear bi-level model with the regional government (leader) aiming to minimize the total risk, while the local government (follower) wished to attain risk equity. Later, Gzara [2013] provided a bi-level multi-commodity network flow model for hazmat transportation, which was then solved by a cutting plane algorithm integrated with several valid cuts.

Although an HTND policy can effectively mitigate the system risk by preventing hazmat shipments from passing through high-risk routes, several limitations make this approach undesirable to hazmat carriers. First, HTND has been criticized as too rigid, due to the ignorance of the carriers' priorities. Second, road closure may cause a waste of available infrastructure resources. Moreover, the policy may not lead to a rational adjustment of the hazmat flows as planned [Marcotte et al., 2009]. Therefore, a more advantageous policy, a toll setting policy, was proposed in the literature. Next we review the studies in this domain.

2.4.2 Toll Pricing Control for Hazmats

The toll setting policy was originally used for the ordinary traffic control problem. Labbé et al. [1998] proposed a bi-level model, where the government hoped to maximize their profits gained by placing tolls on certain road segments, while the carriers wanted to minimize their total transportation cost. Dial [1999] proposed a model for minimal-revenue tolls in a network with a single origin. Then a fast algorithm was developed to solve this model. Brotcorne et al. [2001] extended the work of Labbé et al. [1998] to a multicommodity case, and a robust algorithm was proposed to solve toll setting problems of significant size. Yildirim and Hearn [2005] introduced a general toll pricing model, which could solve both elastic demand traffic assignment and combined

distribution-assignment problems.

Although toll pricing has been well developed for regular traffic control, it is newly proposed in the hazmat transportation field. The first toll setting policy (TS) for hazmat was proposed by Marcotte et al. [2009] with a bi-level model. When tolls are imposed on populated road segments, carriers are more willing to choose less-populated roads based on economic considerations. In the upper level, an objective function is used to integrate the population exposure with travel cost in deciding the toll policy.

Bianco et al. [2015] introduced a toll setting policy to mitigate the risk generated by hazardous material transportation. This bi-level model was a mathematical programming with equilibrium constraints (MPEC) problem, where the upper-level problem decided the appropriate tolls to minimize both the total network risk and the maximum link risk among the network links (i.e. ensuring risk equity). The lower level problem was formulated as a Nash game among carriers to minimize the transportation cost (including tolls).

The toll setting policy can also be used for other transportation modes. Assadipour et al. [2016] proposed a bi-level bi-objective model to deter the hazmat carriers from using certain terminals in a rail-truck intermodal network. A hybrid speed-constrained multi-objective particle swarm metaheuristic was developed to solve this optimization model.

Another group of studies within the toll-setting domain, dual toll pricing, considers not only the hazmat shipments but also the congestion caused by the regular traffic, which may result in a higher incident rate. Because of the direct connection to our research, we provide a comprehensive review of this policy next.

2.5 Dual Toll Pricing

Wang et al. [2012] introduced a single level dual toll pricing model with the motivation of controlling both regular and hazmat traffic to mitigate the risk. Considering a duration-population-frequency of hazmat exposure, their model incorporated a linear travel delay function to measure risk. This new method can simultaneously control both regular and hazmat flows. Esfandeh et al. [2016] formulated the dual toll problem as a bi-level model with a non-linear travel delay function used by the U.S. Bureau of Public Roads. The upper level minimized the total risk to find both regular and hazmat toll vectors, while the lower level minimized the total cost of the regular vehicles and hazmat carriers. By not ignoring carriersâĂŹ decisions, the bi-level structure made this model more realistic.

We consider our research problem to be an extension of the model proposed by Esfandeh et al. [2016]. Major differences and improvements are addressed as follows. First, at the upper level, apart from the total network risk, we also consider the risk equity as another objective function. Thus, our model allows the local and regional governments to work together and seek a more rational way of properly determining the values of tolls. Second, at the lower level, rather than minimizing only the hazmat carriers' cost, we include the minimization of the transportation cost of the non-hazmat shipments as well. That is because the regular carriers should also have the opportunity to decide their own shipment flows according to the regular toll. Third, rather than only one hazmat carrier with a single type of hazmat, our model allows multiple carriers who transport several types of hazmat. Due to the distinct impacts on the environment, different toll values can be computed through the proposed model. The details regarding our mathematical model are presented in the next chapter.

Chapter 3

Mathematical Model

This chapter contains a detailed description of the research problem (Section 3.1) and the model structure (Section 3.2). Section 3.5 contains our mathematical formulation. This is preceded by the model assumptions (Section 3.3) and a comprehensive list of notation (Section 3.4).

3.1 Problem Definition

Consider a directed network $G = (N, A)$, with a set of nodes N and a set of arcs A. Let v_{ij} be the regular traffic flow on arc (i, j), i.e., the number of vehicles running through this arc. d^w is the demand for O-D pair w in the set of O-D pairs for regular vehicles W, we have

$$v_{ij} = \sum_{w \in W} y_{ij}^w, \ \ \forall (i, j) \in A,$$

where

$$\sum_{j:(i,j)\in A} y_{ij}^{w} - \sum_{j:(j,i)\in A} y_{ji}^{w} = b_i^w, \ \forall i \in N, \forall (i,j) \in A; \forall w \in W.$$

Note that $b_i^w = d^w$ if node i is the origin of O-D pair w; $b_i^w = -d^w$ if node i is the destination of O-D pair w; and $b_i^w = 0$, otherwise.

Let τ_{ij} be the toll charged to a regular vehicle on arc (i, j). We define the regular cost as:

$$\sum_{(i,j)\in A} (\alpha C_{ij}(v_{ij}) + \tau_{ij}) v_{ij},$$

where C_{ij} is the travel time on arc (i, j), and α is the parameter converting time units into transportation cost units as perceived by regular vehicles. According to Litman [2012], who estimated the travel cost for a regular vehicle, α is \$ 20.44/hr considering fuel, maintenance and insurance cost. The travel time on each arc, given the flow, is defined on the basis of the US Bureau of Public Roads (BPR) function, i.e.,

$$C_{ij}(v_{ij}) = C_{ij}^0 \Big(1 + 0.15 \Big(\frac{v_{ij}}{l_{ij}}\Big)^4\Big), \tag{3.1}$$

where C_{ij}^0 and l_{ij} denote the free travel time and the capacity of arc (i, j), respectively. Note that usually in a road network, the hazmat flow is relatively small compared to the regular flow, and thus it is ignored in this function.

Similarly for the hazmat flow, let $S(m, h)$ be the set of hazmat shipments of carrier m with hazmat type h, n^s the number of trucks for hazmat shipment $s \in S(m, h)$. x_{ij}^s is a binary routing variable indicating whether the shipment s is on arc (i, j). We have

$$\sum_{j:(i,j)\in A} x_{ij}^{s} - \sum_{j:(j,i)\in A} x_{ji}^{s} = e_i^s, \ \forall i \in N, \forall (i,j) \in A; \forall s \in S(m,h),$$

where $e_i^s = 1$ if node i is the origin of the O-D pair on which shipment s is transported; $e_i^s = -1$ if node i is the destination of that shipment; and $e_i^s = 0$, otherwise.

Suppose t_{ij} is the toll charged to a hazmat vehicle on arc (i, j). We define the transportation cost for hazmat shipments as:

$$\sum_{s \in S(m,h)} \sum_{(i,j) \in A} \Big(\beta C_{ij}(v_{ij}) + t_{ij} \Big) n^s x_{ij}^s,$$

where parameter β converts time units into transportation cost units of hazmat vehicles. Park et al. [2014] estimate β to be \$ 24.44/hr, assuming the same cost factors as Litman [2012].

Now consider the risk on arc (i, j). From Table 2.1, as in Batta and Chiu [1988], that can be formulated as:

$$\sum_{s \in S(m,h)} C_{ij}(v_{ij}) \rho_{ij}^h x_{ij}^s n^s,$$

where ρ_{ij}^h is the number of people exposed on arc (i, j) when a hazmat incident occurs. To ensure the equity of the spatial distribution of risk, one of our objectives is to minimize the maximum risk on any link. The upper level problem can be written as

$$\min \Lambda,$$

subject to:

$$\sum_{s \in S(m,h)} C_{ij}(v_{ij}) \rho_{ij} x_{ij}^s n^s \leq \Lambda, \qquad \forall (i, j) \in A.$$

It should be kept in mind that there are multiple valid tolls, hence we add another term to the above objective function to choose the set of tolls with the minimum total value.

Therefore, this objective function can be rewritten as:

$$\min_{t_{ij},\tau_{ij}} \Lambda + \eta \sum_{(i,j)\in A} \big(t_{ij} + \tau_{ij}\big),$$

where the constant η converts the total toll cost to the risk. Note that the value of this constant should be small ($0 \leq \eta \leq 1$), such that the toll term does not overly impact the final solution of the risk.

Similarly, considering all arcs on the network, the total risk is:

$$\sum_{(i,j)\in A} \sum_{s\in S(m,h)} C_{ij}(v_{ij}) \rho_{ij}^{h} x_{ij}^{s} n^{s}.$$

Taking into account the total toll value, the objective function for the total risk can be expressed as:

$$\min_{t_{ij},\tau_{ij}} \sum_{(i,j)\in A} \sum_{s\in S(m,h)} C_{ij}(v_{ij}) \rho_{ij}^{h} x_{ij}^{s} n^{s} + \eta \sum_{(i,j)\in A} \big(t_{ij} + \tau_{ij}\big),$$

3.2 Model Structure

Figure 3.1 depicts the bi-level structure of the proposed model. As shown, three distinct parties are considered: the regional/local government, the non-hazmat travelers and the hazmat carriers (various carriers shipping multiple hazmats). Note that in the upper level, we combine the two levels of government because they need to work with each other to make the decision of setting the tolls, despite their differences in objectives. (The trade-off between these two objectives is a major analysis in our research.) Then in light of the tolls posed by the government, the non-hazmat travelers and hazmat carriers determine their own corresponding shipping flows, aiming to minimize the total

transportation cost. These flows, in turn, influence the government's decisions.

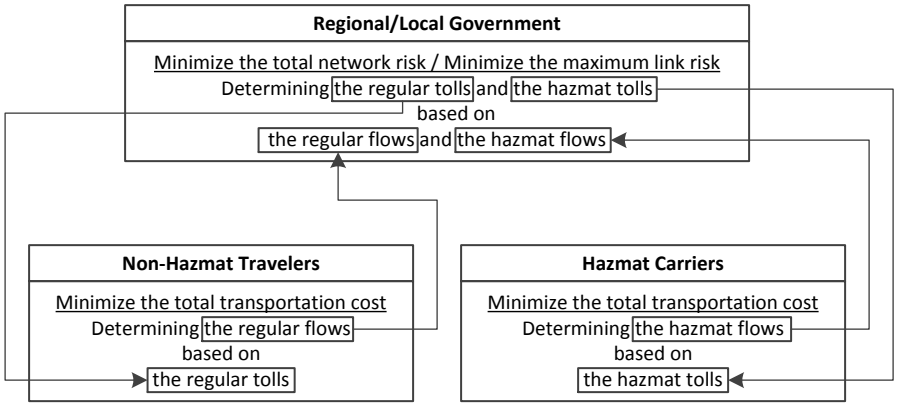

Figure 3.1: Bi-level Structure

3.3 Assumptions

Three assumptions pertain to our model:

1) The flow of hazmat traffic is negligible compared to the number of regular vehicles. As a result, we can say hazmat traffic has no influence on congestion;

2) We assume all involved parties have perfect information about the current status of the network and the cost structure of other parties;

3) We consider a deterministic model, i.e. there is no uncertainty in the network parameters, the travel cost and the behaviors of users;

4) The competition between different hazmat carriers is ignored.

3.4 Notation

In this section, we introduce the notation employed in our research.

Sets

N:	set of nodes, indexed by i and j.
A:	set of arcs.
W:	set of O-D pairs for regular vehicles, whose elements are indicated by w.
M:	set of hazmat carriers, indicated by $m \in M$.
H:	set of hazmat types, $h \in H$.
$S(m,h)$:	set of hazmat shipments for carrier m and hazmat type h, whose typical element is s.

Variables

τ_{ij}:	toll charged to regular vehicles on arc (i,j).
y_{ij}^{w}:	flow of regular vehicles on arc (i,j) for O-D pair w.
v_{ij}:	total traffic of regular vehicles on arc (i,j).
t_{ij}^{h}:	toll charged to vehicles transporting hazmat type h on arc (i,j).
x_{ij}^{s}:	1, if arc (i,j) is used for shipment s; 0, otherwise.

Parameters

d^{w}:	demand of regular vehicles for O-D pair w.
n^{s}:	number of trucks for hazmat shipment s.
C_{ij}:	a nonnegative arc travel time for each arc $(i,j) \in A$.
ρ_{ij}^{h}:	number of people exposed on arc (i,j) when an accident of hazmat type h occurs.

α: a parameter converting time units into transportation cost units perceived by regular vehicles.

β: a parameter converting time units into transportation cost units perceived by hazmat trucks.

η: coefficient of the overall sum of tolls.

ϱ: maximum value of regular toll on any arc.

π: maximum value of hazmat toll on any arc.

3.5 Mathematical Formulation

The upper level model [UL] is:

$$\min_{t_{ij}^h, \tau_{ij}} \sum_{s \in S(m,h)} \sum_{(i,j) \in A} C_{ij}(v_{ij}) \rho_{ij}^h x_{ij}^s n^s + \eta \sum_{(i,j) \in A} \left(\sum_{h \in H} t_{ij}^h + \tau_{ij} \right), \tag{3.2}$$

$$\min_{t_{ij}^h, \tau_{ij}} \Lambda + \eta \sum_{(i,j) \in A} \left(\sum_{h \in H} t_{ij}^h + \tau_{ij} \right) \tag{3.3}$$

Subject to:

$$\sum_{s \in S(m,h)} C_{ij}(v_{ij}) \rho_{ij}^h x_{ij}^s n^s \leq \Lambda, \forall (i,j) \in A, \tag{3.4}$$

$$\tau_{ij} \leq \varrho, \forall (i,j) \in A, \tag{3.5}$$

$$t_{ij}^h \leq \pi, \forall (i,j) \in A, \forall h \in H, \tag{3.6}$$

The lower level model [LL] is:

$$\arg\min_{v_{ij},x_{ij}} \sum_{(i,j)\in A} \Big(\alpha C_{ij}(v_{ij}) + \tau_{ij}\Big)v_{ij} + \sum_{s\in S(m,h)} \sum_{(i,j)\in A} \Big(\beta C_{ij}(v_{ij}) + t_{ij}^{h}\Big)n^{s}x_{ij}^{s} \tag{3.7}$$

Subject to:

$$v_{ij} = \sum_{w\in W} y_{ij}^{w},\ \ \forall (i,j)\in A, \tag{3.8}$$

$$\sum_{j:(i,j)\in A} y_{ij}^{w} - \sum_{j:(j,i)\in A} y_{ji}^{w} = b_{i}^{w},\ \ \forall i\in N, \forall (i,j)\in A; \forall w\in W, \tag{3.9}$$

$$\sum_{j:(i,j)\in A} x_{ij}^{s} - \sum_{j:(j,i)\in A} x_{ji}^{s} = e_{i}^{s},\ \ \forall i\in N, \forall (i,j)\in A; \forall s\in S(m,h), \tag{3.10}$$

$$v_{ij}\ integer,\ \ \forall (i,j)\in A, \tag{3.11}$$

$$x_{ij}^{s}\in 0,1,\ \ \forall (i,j)\in A; \forall s\in S(m,h). \tag{3.12}$$

This is a bi-level model. In the upper level model [UL], two objective functions are mentioned: Objective (3.2) minimizes the total network risks, and objective (3.3) minimizes the maximum link risk. In other words, objective (3.3) ensures risk equity. Note that an additional term, the total toll costs, is added to both objectives. As mentioned, there can be multiple valid tolls, and we want to choose tolls with minimum value. The coefficient, η, is associated with the total-toll-cost terms. As explained in Section 3.1, constraint (3.4) plus objective (3.3) enable proper calculation of risk equity.

In the lower level model [LL], objective (3.7) minimizes the total transportation costs, including the costs for both regular and hazmat shipments. It will be important,

later, to note that the second portion of the lower level objective (3.7), i.e., the hazmat transportation cost, is non-convex. Constraints (3.8) to (3.10) ensure the flow balance of the network.

Due to the non-linear and bi-level nature of this formulation, no pre-designed optimization algorithm is workable. Therefore, we propose a solution procedure in the next chapter based on a metaheuristic to resolve this issue.

Chapter 4

Solution Methods

The major complications in solving our model lie in two aspects: 1) it is difficult to find the optimal solution for a bi-level model, and 2) the lower level objective function contains non-linear terms. Normally, it is hard to solve bi-level models because of the challenge in calculating the upper level objective function and the interaction between the problems at each level. In this research, we present a genetic-algorithm based solution procedure to generate optimal solutions. Two different methods, a piecewise linearization approach [Wang et al., 2012] and the Frank-Wolfe algorithm [Frank and Wolfe, 1956], will each be applied to our lower level problem. These processes are discussed in detail next.

4.1 Genetic Algorithm (GA)

The genetic algorithm is a metaheuristic method motivated by the process of natural selection. Based on the assumption that better parents usually generate better offspring, candidate solutions, represented by chromosomes, evolve through crossover and mutation

Algorithm 4.1 Genetic Algorithm for bi-level model

define chromosomes respectively for regular and hazmat shipments on each arc
calculate fitness value (upper-level objective function)
    substitute the value of toll vectors into lower level
    use linearization approach or the Frank-Wolfe algorithm to find regular and hazmat flow
    substitute network flow into upper level and calculate objective function
while $(i \leq Maximum\ Generation)$ and $(j \leq Maximum\ consecutive\ times)$ **do**
  use roulette wheel selection to select parents
  two-point crossover
  one-point mutation
  calculate fitness value of resulting children with linearization approach or the Frank-Wolfe algorithm
  compare the fitness value of resulting children with the population pool, and the inferior solutions are discarded.
  return toll vectors for regular travelers and hazmat carriers

toward better solutions to an optimization model. Among all metaheuristics, GA is regarded as a practical approach for three reasons. First, it is easy to understand and apply to a model. Second, with an intrinsically parallel searching scheme, near-global optimal solutions can be found in a reasonable time. Third, a genetic algorithm is more likely to find a global optimal solution because of its large starting population and proper selection mechanism. The flowchart in Figure 4.1 shows the general procedure of a GA, and Algorithm 4.1 describes how GA is applied in our case. In the following sections, we provide detailed explanations of the major steps in this algorithm.

4.1.1 Encoding and Decoding

In GA, a chromosome, consisting of a set of values, represents a feasible solution. Considering the nature of our problem, we define the chromosomes respectively for the regular and hazmat shipments on each arc (Figure 4.2). The value of each gene is the toll

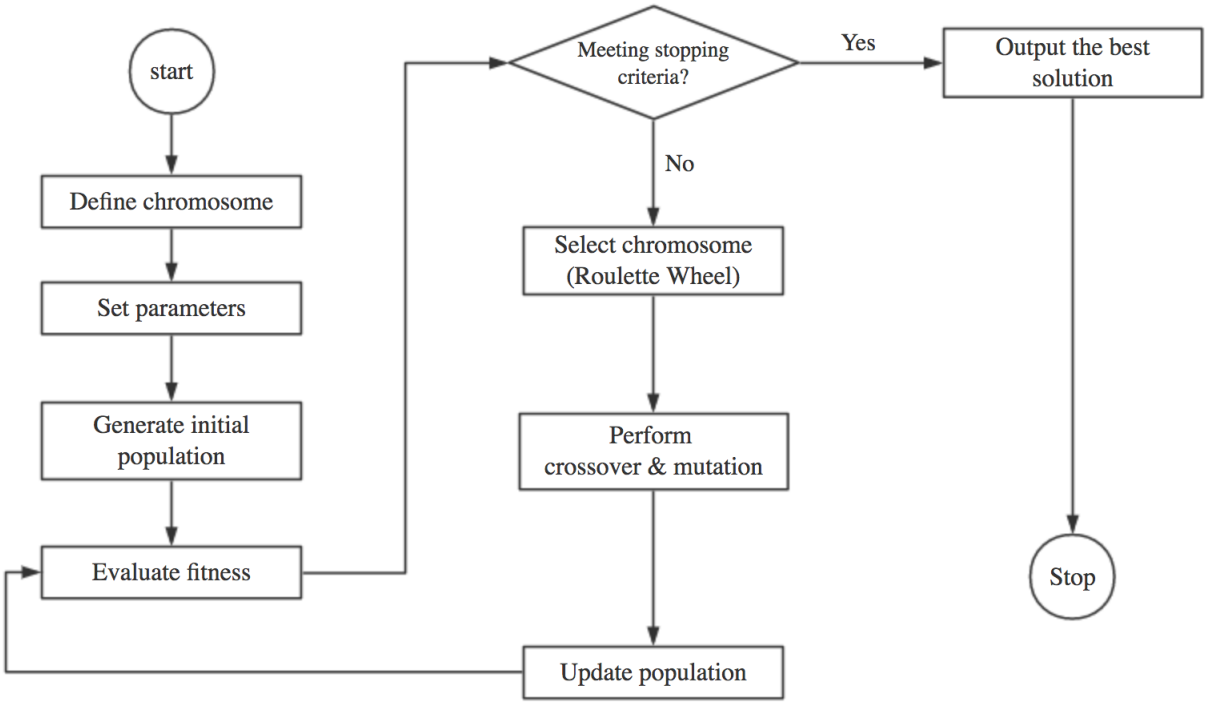

Figure 4.1: Genetic algorithm

value for the corresponding arc, and the length of the chromosome is the number of arcs in the existing network.

	Arc 1	Arc 2	...	Arc a	...	Arc n-1	Arc n
Chromosome – regular toll	τ_1	τ_2	⋯	τ_a	⋯	τ_{n-1}	τ_n
Chromosome – hazmat toll	t_1	t_2	⋯	t_a	⋯	t_{n-1}	t_n

Figure 4.2: Chromosomes

4.1.2 Selection

Roulette wheel selection is implemented to choose parents for generating children. Each chromosome is assigned to a slice of the wheel, and the size of that slice depends on its fitness value. By doing so, a chromosome that is more fit has a greater chance to be selected than one that is less fit. The procedure is presented as follows:

1. Calculate the total fitness value: sum the fitness values for all chromosomes in the selected population, and let the total fitness value be T.

2. Calculate the cumulative probability: given that the probability of chromosome i is equal to its fitness value divided by T, sum the first i probabilities for chromosome i.

3. Repeat N times (N is the number of chromosomes to be selected)

1). randomly generate a number r between 0 and 1.

2). compare r and the cumulative probability. Select that chromosome whose cumulative probability is the first one larger than r.

4.1.3 Crossover

The crossover operator is used to generate offsprings from the selected parents. In our model, we employ a two-point crossover. First, we randomly generate a number between 0 and 1. [That is, from the uniform distribution on the interval (0, 1).] If this random number is smaller than the crossover rate γ, a crossover is performed; otherwise, we keep the original genes of the parents. (The effect of different crossover rates is analyzed in the next chapter. Based on that analysis, a crossover rate of 0.8 is used in the solution procedure.)

To actually conduct the crossover, an additional two random numbers are generated, to indicate the starting and ending position of the crossover. (These discrete random numbers are uniformly distributed over the interval (1, $|A|$), where $|A|$ is the cardinality of the set A of all arcs in the network.) Every gene between these two positions is swapped, while all other genes stay the same. The resulting chromosomes are the offsprings. Figure 4.3 gives a sample illustration, where the discrete uniform random numbers were 4 and 6.

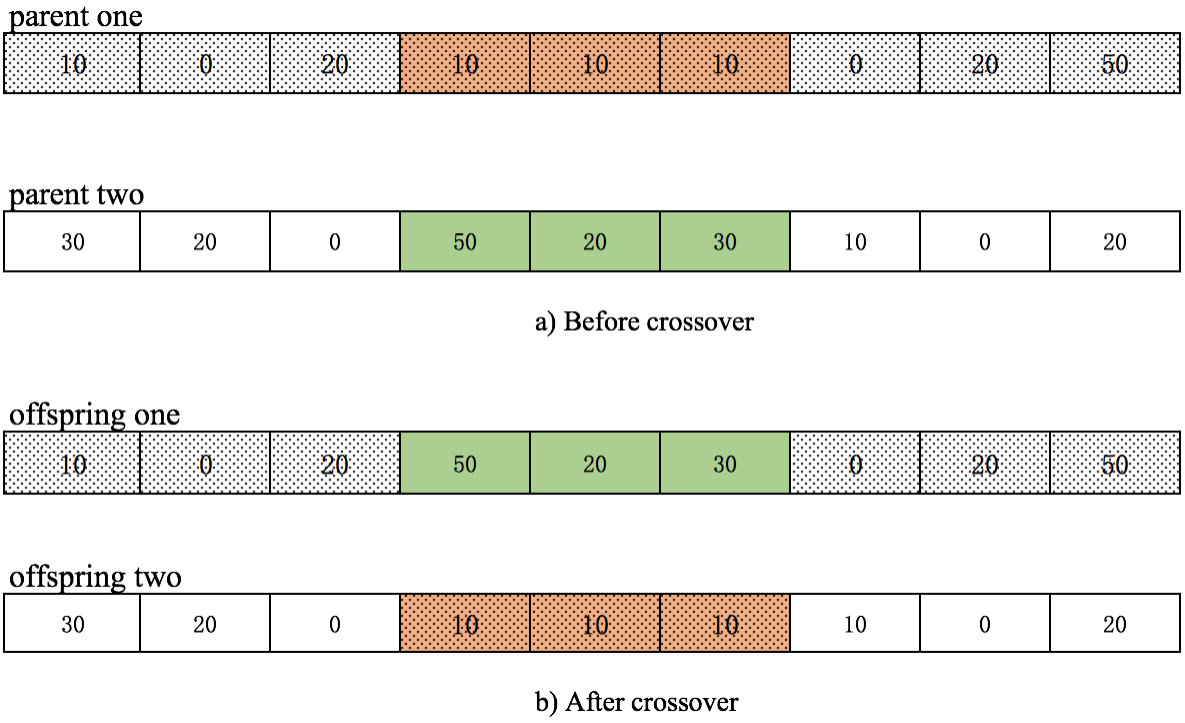

Figure 4.3: Crossovers

4.1.4 Mutation

Mutation is important in maintaining diversity from one generation to the next, and thus is necessary to escape from local optima. In this research, we implement a one-point

mutation with a mutation rate of $\zeta = 0.03$. This value is tested in the next chapter.

A random number is generated between 0 and 1 for each chromosome. If this random number is less than ζ, we perform mutation; otherwise, we do nothing. In the case of mutation, the position of the mutated gene is also randomly generated; the value after mutation can be a random integer within the feasible range of the tolls. A sample mutation is given in Figure 4.4, for the simple case in which the tolls can range between 0 and 50.

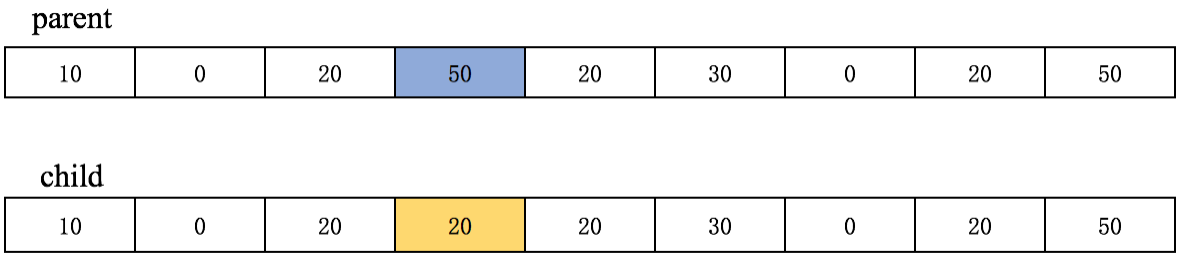

Figure 4.4: Mutation

4.1.5 Fitness Value

In solving our bi-level model, the fitness value refers to the objective function value at the upper level. Given the bi-objective nature of the proposed model, we employ the weighted sum method to integrate the two objectives to a single objective. The application of weights is the most commonly used approach in bi-objective optimization, due to the simplicity in examining the trade-offs between the two objectives. Hence, the weights corresponding to the total risk and the risk equity are varied later in the next chapter. That will reveal the relationships between those two objectives, and how they impact the network flows and the dual toll policy.

In this research, the fitness evaluation connects the upper and lower levels. In particular, the chromosomes containing toll information are treated as known parameters and passed to the lower level model. Solution of the latter yields the optimal flows, for both regular and hazmat shipments, on each arc. Those flows are then used to calculate the weighted objective function for fitness evaluation.

Note that the non-linear terms in the lower level objective function cause additional difficulty in optimization. We therefore adopt a piece-wise linearization method or the Frank-Wolfe algorithm to resolve this complication.

4.1.6 Termination

Two stopping criteria are considered in our algorithm:

1) number of generations, and

2) number of iterations without convergence

These two rules are tested in the next chapter to show the impact on the rate of convergence.

4.2 Piecewise Linearization (PL)

Recall that the hazmat transportation cost portion of Eq. (3.7) is a non-convex function. This makes the lower level model a non-convex problem, and complicates its optimization. In this section, we show in detail how the regular and hazmat cost functions can be linearized. The linearization procedure is adapted from Wang and Lo [2010] with certain modifications.

4.2.1 Regular Flow

First, let us recall the cost to regular traffic users in the lower level model:

$$\Pi_v = \sum_{(i,j)\in A} (\alpha C_{ij}(v_{ij}) + \tau_{ij}) v_{ij}, \tag{4.1}$$

where $C_{ij}(v_{ij}) = C_{ij}^0 \Big(1 + 0.15 \Big(\frac{v_{ij}}{l_{ij}}\Big)^4\Big)$.

For illustrative purposes and notational simplicity, let $A_a = C_a^0$ and $B_a = 0.15 C_a^0/(l_a)^4$ where $a \in A$ denotes arc (i, j). We consider the BPR travel time function expressed as:

$$C_a(v_a) = A_a + B_a(v_a)^4, \tag{4.2}$$

where v_a denotes the traffic volume on each arc a ∈ A. v_a is the only decision variable. Next, we represent this link travel time function as a piecewise-linear function.

Let the feasible domain of v_a (i.e. $[0, \overline{v_a}]$) be partitioned into N segments. For each arc a, we choose a series of values of $K_{a,n}$ to partition the feasible domain of v_a into a number of small regions, where $0 < K_{a,n} \leq v_a < K_{a,n+1} < \overline{v_a}$ for $n = 1, ..., N-1$. It is easy to see that, the smaller the region, the more precise will be the results.

However, we also take computation time into consideration. If the region is too small, the time will be much longer. Letting $F_a(v_a) = (\alpha C_a(v_a) + \tau_a) v_a = (\alpha(A_a + B_a(v_a)^4) + \tau_a) v_a$, we can specify a linear function to approximate $F_a(v_a)$ within a given region, i.e.,

$$F_a(v_a) \approx \mu_n^a v_a + \nu_n^a, \text{ if } K_{a,n} \leq v_a < K_{a,n+1}, \tag{4.3}$$

with μ_n^a and ν_n^a denoting the parameters of the linear function. To find those parameters,

we use a first-order Taylor expansion of $F_a(v_a)$. That is, when $K_{a,n} \leq v_a < K_{a,n+1}$, parameters μ_n^a and ν_n^a can be approximated by the partial derivatives of $F_a(v_a)$ with respect to v_a evaluated at $K_{a,n}$, as follows:

$$\mu_n^a = \left.\frac{\partial F_a}{\partial v_a}\right|_{K_{a,n}} = 5\alpha B_a (K_{a,n})^4 + (\alpha A_a + \tau_a), \text{ and thus} \tag{4.4}$$

$$\nu_n^a \approx F_a(K_{a,n}) - K_{a,n} \left.\frac{\partial F_a}{\partial v_a}\right|_{K_{a,n}} = -4\alpha B_a (K_{a,n})^5. \tag{4.5}$$

It is easy to see that, once we fix the region in which v_a falls, μ_n^a and ν_n^a become known parameters. Eq. (4.3) then becomes a linear function in v_a. Replacing Eq. (4.3) in Eq. (4.1), the latter is now transformed to a linear form:

$$\sum_{a \in A} (\mu_n^a v_a + \nu_n^a). \tag{4.6}$$

To account for this linear approximation of $F_a(v_a)$, and the preceding non-convexity, the following constraints must be added to the original model.

$$L\delta_{a,n} \leq v_a - K_{a,n} \leq U(1 - \delta_{a,n}) - \epsilon, \qquad \forall a, \forall n, \tag{4.7}$$

$$\gamma_{a,n} = \delta_{a,n+1} - \delta_{a,n}, \qquad \forall a, \forall n, \tag{4.8}$$

$$L(1 - \gamma_{a,n}) \leq F_a - (\mu_n^a v_a + \nu_n^a) \leq U(1 - \gamma_{a,n}), \qquad \forall a, \forall n, \tag{4.9}$$

$$\delta_{a,n}, \gamma_{a,n} \in \{0, 1\}, \qquad \forall a, \forall n, \tag{4.10}$$

$$F_a \geq 0, \qquad \forall a, \tag{4.11}$$

$$n = 1, ..., N, \tag{4.12}$$

$$a \in A, \tag{4.13}$$

$$s \in S. \tag{4.14}$$

In the above constraints, L and U represent very large negative and very large positive constants, respectively, and ϵ is a very small positive constant. $\delta_{a,n}$ denotes a binary variable indicating whether v_a is greater than $K_{a,n}$ or not: $v_a \in [K_{a,n}, \infty)$ if $\delta_{a,n} = 0$; $v_a \in [0, K_{a,n})$ otherwise; this can be verified by Eq. (4.7). Another binary variable $\gamma_{a,n}$, defined as the difference between $\delta_{a,n}$ and $\delta_{a,n+1}$, determines whether v_a falls in the segment $[K_{a,n}, K_{a,n+1})$ or not: in other words, $\gamma_{a,n}$ expresses the two conditions wherein $\delta_{a,n} = 0$ and $\delta_{a,n+1} = 1$, implying that $v_a \in [K_{a,n}, K_{a,n+1})$. For the other possible combinations of $\delta_{a,n}$ and$\delta_{a,n+1}$, we have $\gamma_{a,n}$ which represents the situation $v_a \notin [K_{a,n}, K_{a,n+1}]$.

Suppose v_a lies in the region $[n]$. Substituting $\gamma_{a,n} = 1$ into Eq. (4.9), we have:

$$0 \leq F_a - (\mu_n^a v_a + \nu_n^a) \leq 0 \Leftrightarrow F_a = (\mu_n^a v_a + \nu_n^a). \tag{4.15}$$

Therefore, the optimization model for the regular flow can be linearized as:

$$\min \Pi_v = \sum_{a \in A} F_a(v_a)$$

Subject to: $v \in V$, and Eqs. (4.3) to (4.5) and (4.7) to (4.14).

4.2.2 Hazmat Flow

The non-linear objective function for hazmat flow is:

$$\Pi_x = \sum_{s \in S(m,h)} \sum_{(i,j) \in A} (\beta C_{ij}(v_{ij}) + t_{ij}^h) x_{ij}^s n^s. \tag{4.16}$$

The linearization approach consists of two steps. The first step is to linearize the traffic-time function; that function and its linearization are exactly the same as for the regular flow.

Let $G_a(v_a) = \beta C_{ij}(v_{ij}) + t^h_{ij}$. Just as in Eq. (4.3) for the regular flow, we can specify a linear function to approximate $G_a(v_a)$ within each region. That is,

$$G_a(v_a) \approx \kappa^a_n v_a + \omega^a_n, \tag{4.17}$$

if $K_{a,n} \leq v_a < K_{a,n+1}$, where κ^a_n and $\omega^{a,h}_n$ denote the parameters of that linear function. Then, we have

$$\kappa^a_n = \left.\frac{\partial G_a}{\partial v_a}\right|_{K_{a,n}} = 4\beta B_a(K_{a,n})^3, \text{ and} \tag{4.18}$$

$$\omega^{ah}_n = G_a(v_a) - K_{a,n}\left.\frac{\partial G_a}{\partial v_a}\right|_{K_{a,n}} = (\beta A_a + t^h_a) - 3\beta B_a(K_{a,n})^4. \tag{4.19}$$

Substituting Eq. (4.17) in Eq. (4.16), the cost function to be minimized is transformed to the following:

$$\sum_{s\in S(m,h)}\sum_{a\in A}(\kappa^a_n v_a + \omega^{ah}_n)x^s_a n^s. \tag{4.20}$$

In addition, let us introduce a new variable $G_a(v_a, x^s_a)$, for all arcs $a \in A$ and shipments $s \in S(m,h)$. That new variable denotes the travel time on arc a, incorporating the decisions of both types of traffic. Specifically:

$$G_a(v_a, x^s_a) = \kappa^a_n v_a x^s_a + \omega^{ah}_n x^s_a, \text{ if } K_{a,n} \leq v_a < K_{a,n+1}. \tag{4.21}$$

Note that Eq. (4.21) is the extended form of $G_a(v_a, x_a^s) = G_a(v_a)x_a^s$ with $G_a(v_a)$ replaced by its linear-function approximation. When arc a is used by hazmat shipment s, i.e., $x_a^s = 1$, $G_a(v_a, x_a^s)$ equals the arc travel time, $\kappa_n^a v_a + \omega_n^{ah}$; otherwise, with $x_a^s = 0$, and any regular traffic flow v_a, $G_a(v_a, x_a^s)$ equals 0.

To account for this linear approximation of $G_a(v_a)$, the following constraints must be added to the original model.

$$L\delta_{a,n} \leq v_a - K_{a,n} \leq U(1 - \delta_{a,n}) - \epsilon, \qquad \forall a, \forall n, \tag{4.22}$$

$$\gamma_{a,n} = \delta_{a,n+1} - \delta_{a,n}, \qquad \forall a, \forall n, \tag{4.23}$$

$$L(1 - \gamma_{a,n}) \leq G_a - (\kappa_n^a v_a x_a^s + \omega_n^{ah} x_a^s), \qquad \forall a, n, s, \tag{4.24}$$

$$G_a - (\kappa_n^a v_a x_a^s + \omega_n^{ah} x_a^s) \leq U(1 - \gamma_{a,n}), \qquad \forall a, n, s,$$

$$G_a \geq 0, \qquad \forall a, \tag{4.25}$$

In the above constraints, $L, U, \epsilon, \delta_{a,n}$ and γ share the same meanings as in the regular flow linearization.

When v_a is in the region $[K_{a,n}, K_{a,n+1})$, substituting $\gamma_{a,n} = 1$ into Eq. (4.24), we have:

$$0 \leq G_a - (\kappa_n^a v_a x_a^s + \omega_n^{ah} x_a^s) \leq 0. \tag{4.26}$$

which produces the required simultaneous results in Eq. (4.21). From Eq. (4.20), it is easy to find that, although we have linearized the travel time function $C_a(v_a)$, the transformation of the objective function in Eq. (4.20) still contains bilinear terms, yielding a mixed-integer bilinear program (BLP). Every bilinear term involves the product of a nonnegative integer variable v_a and a binary variable x_a^s.

For each arc a, we define a new integer variable p_a^s, which is represented by the

product of v_a and x_a^s. It will replace the bilinear terms in Eq. (4.20), with the addition of some constraints. Specifically:

$$\{p_a^s : \ p_a^s = v_a x_a^s, \ v_a \leq \bar{v_a}, \ x_a^s \leq 1, \ \forall a \in A, \forall s \in S(m,h)\}. \tag{4.27}$$

The following constraints need to be added to the model.

$$p_a^s \leq \bar{v_a} x_a^s, \qquad \forall s, \forall a, \tag{4.28}$$

$$p_a^s \leq v_a, \qquad \forall s, \forall a, \tag{4.29}$$

$$p_a^s \geq v_a + \bar{v_a} x_a^s - \bar{v_a}, \qquad \forall s, \forall a, \tag{4.30}$$

$$p_a^s \geq 0, \qquad \forall s, \forall a. \tag{4.31}$$

Now, replacing the bilinear term in Eqs. (4.20) and (4.24) with its equivalent continuous variable p_a^s, the non-linearity of the problem is finally removed. The optimization model for the hazmat flow is thus linearized as:

$$\min \Pi_x = \sum_{a \in A} \sum_{s \in S(m,h)} n^s G_a(v_a, x_a^s)$$

Subject to:

Eqs. (4.17) to (4.19), and (4.22) to (4.31).

4.3 Frank-Wolfe Algorithm (FW)

Although the above piecewise linearization approach can solve this non-convex lower level problem, a longer computational time will be needed. For example, in a 15-node

network, when the feasible domain is divided into 100 segements, the computation time is 89,520 seconds. In a 24-node network, even though the partition scheme involves only 10 intervals, no optimal solution could be found within the time limit of 172,800 seconds. (Details about the computation time in the case of piecewise linearization will be shown in Section 5.4.) Therefore, it is unrealistic to apply piecewise linearization to a large-scale, real-world situation. Thus, we suggest an alternative method, the Frank-Wolfe algorithm, which was proposed by Frank and Wolfe [1956]. Detailed comparison of the piecewise linearization approach and the Frank-Wolfe algorithm will be discussed in Section 5.4.

The Frank-Wolfe algorithm was presented in 1956 to apply to quadratic programming, and then was extended to be used in many different areas. For example, Wang and Qian [2016] used this algorithm to solve a biological network problem. Meng et al. [2008] implemented the Frank-Wolfe algorithm for a traffic assignment problem. FW is a popular method for large-scale network problems because of its simple implementation and fast computation time.

Although the Frank Wolfe algorithm can magnificently improve our computation time, there still exist two problems. First, we cannot guarantee that this algorithm can find the global optimal solution for our problem because it is designed for $convex$ optimization problems. In other words, this iterative first-order optimization algorithm may not yield the optimal solution for our non-convex problem. In Section 5.3, we will compare the quality of solutions from the Frank-Wolfe algorithm and the piecewise linearization approach, and show that the approximate solutions we get from the Frank-Wolfe algorithm are efficient for our lower level problem.

Second, our model involves both integer and binary variables, and it is difficult for the Frank-Wolfe algorithm to deal with both types of variables at the same time. Therefore, we initially relax the binary constraints, and get an approximate solution to our lower

level problem with the Frank-Wolfe algorithm. Then, a post iteration is applied to this approximate solution. Details will be discussed in the following.

Now recall the objective function of our lower level problem (3.7):

$$\min_{v\in V, x\in X} z(v,x) = \sum_{(i,j)\in A}\Big(\alpha C_{ij}(v_{ij}) + \tau_{ij}\Big)v_{ij} + \sum_{s\in S(m,h)}\sum_{(i,j)\in A}\Big(\beta C_{ij}(v_{ij}) + t^h_{ij}\Big)n^s x^s_{ij},$$

where $C_{ij}(v_{ij}) = A_{ij} + B_{ij}(v_{ij})^4$.

The objective function (3.7) can be replaced by its first-order Taylor-series approximation at any random point$(\hat{v},\hat{x})$ (a feasible solution of problem (3.7)):

$$z(v,x) \approx z(\hat{v},\hat{x}) + \frac{\partial z}{\partial v}(\hat{v},\hat{x})(v-\hat{v}) + \frac{\partial z}{\partial x}(\hat{v},\hat{x})(x-\hat{x}) + \ldots,$$

Since $z(\hat{v},\hat{x})$, $\frac{\partial z}{\partial v}(\hat{v},\hat{x})\hat{v}$ and $\frac{\partial z}{\partial x}(\hat{v},\hat{x})\hat{x}$ are constant terms, we can ignore them when minimizing the objective function. v_{ij} is subject to constraints (3.8), (3.9), and its objective function is $\min_{v\in V} v^T \dfrac{\partial z(v^k,x^k)}{\partial v}$, while x^s_{ij} is subject to constraints (3.10), and the corresponding objective function is $\min_{x\in X} x^T \dfrac{\partial z(v^k,x^k)}{\partial x}$. Hence, this minimization problem for the Frank-Wolfe algorithm can be rewritten as two separate linear problems, for regular flow and hazmat flow.

For the regular flow (v_{ij}) part of the lower level model [LL], we have:

$$\min_{v\in V} \sum_{(i,j)\in A}(\alpha A_{ij} + \tau_{ij} + 5\alpha B_{ij}(v^k_{ij})^4)v_{ij} + \sum_{s\in S(m,h)}\sum_{(i,j)\in A} 4\beta B_{ij}x^{sk}_{ij}(v^k_{ij})^3 v_{ij}, \tag{4.32}$$

Subject to:

Eqs. (3.8) and (3.9).

For the hazmat flow (x_{ij}^s) portion of [LL], we must solve:

$$\min_{x \in X} \sum_{s \in S(m,h)} \sum_{(i,j) \in A} \left(\beta A_{ij} + t_{ij}^h + \beta B_{ij} (v_{ij}^k)^4 n^s x_{ij}^s\right), \tag{4.33}$$

Subject to:

$$\text{Eqs. (3.10)},$$

where (v^k, x^k) denotes the solution of $z(v, x)$ at iteration k.

Now, we state the steps of the Frank-Wolfe algorithm for solution of the nonlinear model [LL].

Step 0: Begin with a feasible solution of problem (3.7). Here (v^k, x^k) represents our starting point, and set k to 0 at first;

Step 1: Let m^k and n^k denote the solutions to problem (4.32) and problem (4.33), respectively;

Step 2: Search directions: for regular flow, $d_v^k = m^k - v^k$; for hazmat flow, $d_x^k = n^k - x^k$;

Step 3: Substitute $(v^k + \omega_k d_v^k, x^k + \omega_k d_x^k)$ into problem (3.7) to obtain the step size ω_k. Since this is a one-dimensional problem, a search algorithm, such as the golden section, can be used to solve it.

$$\min z(v^k + \omega_k d_v^k, x^k + \omega_k d_x^k)$$

Subject to:

$$0 \leq \omega_k \leq 1.$$

Then we set,

$$v^{k+1} = v^k + \omega_k d_v^k,$$
$$x^{k+1} = x^k + \omega_k d_x^k.$$

Step 4: Terminate if

$$\left|z(v^{k+1}, x^{k+1}) - z(v^k, x^k)\right| / z(v^k, x^k) \leq \chi,$$

where χ is set to be 0.0001 in our model. Otherwise, increase k by one. Replace (v^k, x^k) with the new solution (v^{k+1}, x^{k+1}), and go to Step 1.

We set $\tilde{v} \in V$ and $\tilde{x} \in X$ to denote the approximate solution to [LL] after using the Frank-Wolfe algorithm. Then we apply the post-iteration to $(\tilde{v}, \tilde{x})$, as follows:

$$\tilde{v}^{l+1} = arg \min_{v \in V} z(v, \tilde{x}^l), \tag{4.34}$$

$$\tilde{x}^{l+1} = arg \min_{x \in X} z(\tilde{v}^{l+1}, x). \tag{4.35}$$

This continues until convergence. We begin with an initial solution $\tilde{x}^l = \tilde{x}$ when $l = 0$, and the objective function for regular flow problem (4.34) is:

$$\min_{v \in V} \sum_{(i,j) \in A} (\alpha A_{ij} + \alpha B_{ij} (v_{ij})^4 + \tau_{ij}) v_{ij} + \sum_{s \in S(m,h)} \sum_{(i,j) \in A} \beta B_{ij} (v_{ij})^4 n^s \tilde{x}_{ij}^s. \tag{4.36}$$

Obviously, this is a typical convex traffic assignment problem with only regular flow variables, which can be easily solved by the Frank-Wolfe algorithm. Detailed procedures are now stated:

First, we solve problem (4.36) to get the regular flow.

Step 0: Select $\tilde{v}^l$ as the starting feasible solution for (4.36). l denotes the number of the iteration, and when $l = 0$, $\tilde{v}^l = \tilde{v}$;

Step 1: For the regular flow, the first-order Taylor approximation at $\tilde{v}^l$ would be:

$$\min_{v\in V} r(v) = \min_{v\in V} \sum_{(i,j)\in A} (\alpha A_{ij} + 5\alpha B_{ij}(\tilde{v}^l)^4 + \tau_{ij})v_{ij} + \sum_{s\in S(m,h)} \sum_{(i,j)\in A} 4\beta B_{ij}(\tilde{v}^l)^3 n^s \tilde{x}^s_{ij} v_{ij}. \quad (4.37)$$

Let $\tilde{p}^l$ denote the solution to problem (4.37);

Step 2: Search direction:

$$d^l = \tilde{p}^l - \tilde{v}^l;$$

Step 3: Step size λ_l is obtained by solving the following one dimensional problem at each iteration.

$$\min r(\tilde{v}^l + \lambda_l d^l)$$

Subject to:

$$0 \le \lambda_l \le 1.$$

Then we set,

$$\tilde{v}^{l+1} = \tilde{v}^l + \lambda_l d^l;$$

After the first three steps, we find the regular flow, then we substitute $\tilde{v}^{l+1}$ into Eq. (4.35) to get the hazmat flow.

Step 4: Now, 4.35 can be rewritten as:

$$\min_{x\in X} \sum_{s\in S(m,h)} \sum_{(i,j)\in A} \beta B_{ij}(\tilde{v}^{l+1}_{ij})^4 n^s x^s_{ij}. \quad (4.38)$$

This is a shortest path problem, and can be easily solved by the Dijkstra algorithm. Let $\tilde{x}^{(l+1)}$ denote the solution;

Step 5: Terminate, if

$$\left|z(\tilde{v}^{l+1}, \tilde{x}^{l+1} - z(\tilde{v}^{l}, \tilde{x}^{l})\right| / z(\tilde{v}^{l}, \tilde{x}^{l}) \leq \chi, \tag{4.39}$$

where χ is set to 0.0001 as before. Otherwise, increase l by one and choose $(\tilde{v}^{l+1}, \tilde{x}^{l+1})$ as the starting point. Return to Step 1.

Chapter 5

Computational Results

The performance of the proposed solution methods is now evaluated. The suggested algorithms are coded in Python 2.7, and tested on a computer with an i-5 Quad Core processor running at 2.6 GHz and 8 GB of memory. The analyses are organized into five sections: performance illustration, partition scheme analysis, variation of the maximum toll value, trade-off analysis and convergence analysis. Several cases (Table 5.1), based on three networks, with 8 nodes, 15 nodes and 24 nodes, are carried out in this chapter. Both the 8-node and 15-node examples are exactly the same networks used by Esfandeh et al. [2016]. The 24-node network, proposed by Suwansirikul et al. [1987], is based on the roads of the city of Sioux Fall, South Dakota. The same network parameters, such as the link capacity and free-flow travel time, are used as input parameters for the BPR travel time function. The regular demands for each origin and destination (OD) pair are also taken into consideration, as displayed by Suwansirikul et al. [1987] and Esfandeh et al. [2016]. There is no reliable record about multi-hazmat-type shipments for the proposed network models. Thus, inspired by Esfandeh et al. [2016], we randomly generate the origin and destination nodes and the demands for each hazmat shipment.

The population exposure to different hazmats along each link (i, j) is generated based on the data from the respective Census site. Further details on those 8-node, 15-node and 24-node networks can be found in Appendix A.

For the 8-node and 15-node instances, we solve the lower level problem with piecewise linearization. Recall that this approach guarantees the global optimum, and here the computing time is reasonable. For the 24-node network, however, the Frank-Wolfe algorithm is used because of its higher efficiency in calculation.

Table 5.1: List of Cases

Case Number	# Nodes	# Arcs	# regular demands	Hazmat Shipments		
				# hazmat demands	# hazmat types	# carrier types
8-1	8	13	6	2	1	1
8-2			12	4	2	1
8-3			27	6	2	2
8-4			27	15	2	2
15-1	15	28	6	2	1	1
15-2			12	4	2	1
15-3			27	6	2	2
15-4			54	6	2	2
24-1	24	76	5	2	1	1
24-2			10	4	2	1
24-3			25	6	2	2
24-4			50	8	2	2
24-5			100	10	2	2
24-6			200	12	2	2
24-7			552	20	3	2

In this table, the notation N-b indicates case b of an N-node network.

5.1 Performance Illustration

In order to analyze the effectiveness of the dual-toll policy, we calculate the total risk, equity, regular travel and hazmat travel delay time for the no-toll case. Let $v_{ij}^{no-toll}$ and $x_{ij}^{s(m,h)no-toll}$ denote the regular and hazmat flow under the no-toll case. First, we solve the following problem:

$$\min_{v_{ij},x_{ij}} \sum_{(i,j)\in A} \alpha C_{ij}(v_{ij})v_{ij} + \sum_{s(m,h)\in S(m,h)} \sum_{(i,j)\in A} \beta C_{ij}(v_{ij})n^{s(m,h)}x_{ij}^{s(m,h)},$$

with piecewise linearization or the Frank-Wolfe algorithm, to get $v_{ij}^{no-toll}$ and $x_{ij}^{s(m,h)no-toll}$.

Hence, under the no-toll scenario, the performance of the network is indicated by the following metrics:

$$r(v^{no-toll}, x^{no-toll}) = \sum_{s(m,h)\in S(m,h)} \sum_{(i,j)\in A} C_{ij}(v_{ij}^{no-toll})\rho_{ij}^{h} x_{ij}^{s(m,h)no-toll} n^{s(m,h)}, \tag{5.1}$$

$$e(v^{no-toll}, x^{no-toll}) = \max_{(i,j)\in A} \sum_{s(m,h)\in S(m,h)} C_{ij}(v_{ij}^{no-toll})\rho_{ij}^{h} x_{ij}^{s(m,h)no-toll} n^{s(m,h)}, \tag{5.2}$$

$$D_r(v^{no-toll}) = \sum_{(i,j)\in A} C_{ij}(v_{ij}^{no-toll})(v_{ij}^{no-toll}), \tag{5.3}$$

$$D_h(v^{no-toll}, x^{no-toll}) = \sum_{s(m,h)\in S(m,h)} \sum_{(i,j)\in A} C_{ij}(v_{ij}^{no-toll})n^{s(m,h)} x_{ij}^{s(m,h)no-toll}, \tag{5.4}$$

where r, e, D_r and D_h represent the total risk, equity, regular traffic delay and hazmat traffic delay.

Let (v^*, x^*) denote the optimum flow under the dual toll case; its corresponding best toll vectors (τ^*, t^*) are obtained from the genetic algorithm. To compare the dual-tolled network with one without tolls, the changes in equity, risk, regular traffic delay and

hazmat traffic delay are calculated by the following procedures:

$$\% \text{ Change in Equity} = \frac{e(v^*, x^*) - e(v^{no-toll}, x^{no-toll})}{e(v^{no-toll}, x^{no-toll})} \times 100,$$

$$\% \text{ Change in Total Risk} = \frac{r(v^*, x^*) - r(v^{no-toll}, x^{no-toll})}{r(v^{no-toll}, x^{no-toll})} \times 100,$$

$$\% \text{ Change in Regular Traffic Delay} = \frac{D_r(v^*) - D_r(v^{no-toll})}{D_r(v^{no-toll})} \times 100,$$

$$\% \text{ Change in Hazmat Shipment Delay} = \frac{D_h(v^*, x^*) - D_h(v^{no-toll}, x^{no-toll})}{D_h(v^{no-toll}, x^{no-toll})} \times 100.$$

In addition, for the dual toll case, the average toll costs for both regular drivers and hazmat carriers are also calculated:

$$\text{Average Toll Cost (regular)} = \frac{\sum_{(i,j)\in A} \tau_{ij}^* v_{ij}^*}{\sum_{w\in W} d^w},$$

$$\text{Average Toll Cost (hazmat)} = \frac{\sum_{s(m,h)\in S(m,h)} \sum_{(i,j)\in A} n^s t_{ij}^* x_{ij}^{s(m,h)*}}{\sum_{s(m,h)\in S(m,h)} n^s}.$$

Results of the comparison between the dual-toll and no-toll networks for Cases 8-1 to 24-7 are summarized in Table 5.2. Please note that some average toll costs are larger than the pre-determined maximum toll value for each arc ($200). This is because the averaging over toll cost is done in terms of $demand$, rather than over the arcs. As most demand may pass through more than one arc, the corresponding toll payment may thus exceed the maximum arc toll value. For example, in Case 8-3, the total regular flow vector under the toll policy is 8,039, while the total demand is only 3,450. Hence the computed average toll cost for the regular flow is $204.57, slightly higher than $200.

From Table 5.2, it is clear that, under the dual toll policy, both the maximum arc risk and total risk have been substantially improved. For example, in Case 8-3, the maximum risk equity can be enhanced by up to 56.58%, and total risk decreased by 22.75%. However, the improvements in both total risk and risk equity are achieved at the

Table 5.2: Comparison between dual-tolled and no-tolled network performance

Case No.	% Change of total risk	% Change of risk equity	% Change of Delay		Avg. tolls	
			regular	hazmat	regular	hazmat
8-1	-22.71	-58.76	-1.37	2.42	191.23	104.11
8-2	-38.11	-48.15	-0.46	1.26	109.65	175.07
8-3	-22.75	-55.68	-0.08	1.58	204.57	253.73
8-4	-27.17	-53.53	-0.06	2.54	269.16	283.16
15-1	-37.87	-43.13	-0.01	0.59	152.69	256.22
15-2	-32.68	-56.44	-0.04	1.05	106.55	286.59
15-3	-30.51	-46.82	-0.04	1.38	142.88	206.12
15-4	-35.22	-47.26	-0.02	0.76	277.37	217.84
24-1	-40.00	-11.57	0.00	0.48	197.29	60.00
24-2	-27.89	-31.78	-0.08	0.74	180.32	69.95
24-3	-24.81	-27.93	-0.64	1.65	197.27	132.62
24-4	-38.49	-28.78	-0.51	0.03	134.15	119.47
24-5	-31.60	-44.78	-0.11	0.03	124.64	144.28
24-6	-33.20	-48.26	-0.12	0.01	138.22	136.97
24-7	-48.06	-58.94	-0.24	0.04	149.53	126.11

A weighted sum method is employed to solve the upper level model. Both total risk and maximum link risk have a coefficient of 0.5.

expense of increasing the travel time of hazmat carriers, whereas the regular travel time slightly decreases compared to the no toll case. Various toll fees are paid by each regular driver, enabling him/her to be directed to less risky and congested routes, so as to reduce their travel time. However, for hazmat drivers, the dual toll policy causes them to detour into longer paths not used by regular drivers, thus reducing the possibility of accidents caused by congestion. This explains why hazmat carriers spend more time compared to the no-toll scenario. Besides, the dual toll policy also encourages hazmat carriers to choose that path which can equalize the spatial distribution of risk. As we can see from Table 5.2, the risk equity has improved greatly with the dual toll policy.

Another thing to notice is that, the improvement in risk equity and the reduction in total risk are achieved by collecting tolls from $both$ types of traffic. In the real world, knowing the high risk induced by their hazmat transportation, the companies involved maybe find it appropriate to pay certain amounts of money(tolls) to mitigate that risk. However, the regular drivers may find that unacceptable because their tolls are sometimes more than those of the hazmat carriers. Therefore, to make regular drivers more in favour of this dual toll policy, a larger coefficient may be placed on the total regular toll cost terms for the minimization objective functions in the upper level.

In conclusion, the dual toll policy mitigates the total risk and enhances risk equity by collecting different toll fees on each arc, to direct carriers onto different routes. Hence, this policy provides attractive solutions to the government. For regular drivers, though they need to pay some money, they can reduce their travel delay, and increase the safety of their trips.

A detailed solution based on Case 8-3 is shown in Table 5.3. The risk equity has been enhanced by more than 50 %, and the total risk is improved by 22.75 %. Regular travel time also slightly decreases from 724,069 to 723,491 hours. All these improvements are achieved at the expense of increasing the hazmat carriers' travel time. However, as we can see, not all carriers increase their driving time. For carriers of type one that carry hazmat type one, their transportation times nearly stay the same, both before and after the toll-setting policy, because their flow vectors do not change.

Table 5.3: Detailed solutions of Case 8-3

		Before Toll	After Toll	Change %
Regular	Toll Vectors	-	[150,80,150,160,190,80, 30,60,130,40,0,80,120]	
	Total toll	0	773,640	
	Average toll	0	224	
	Flow Vectors	[679,471,100,780,419,1011,390, 780,1080,720, 369,1031,209]	[671,479,100,780,411,1019,390, 780,1080,720,369,1031,209]	
	Travel Time (h)	724,069	723,491	-0.08 %
Carrier 1 Hazmat 1	Toll Vectors	-	[50,150,190,70,40,20, 0,0,60,140,20,10,160]	
	Total Toll	0	480	
	Average Toll	0	120	
	Flow Vectors S1	[1,0,0,1,0,0,0,0,0,0,0,0,0]	[1,0,0,1,0,0,0,0,0,0,0,0,0]	
	Travel Time (h)	739	739	0.00
Carrier 1 Hazmat 2	Toll Vectors	-	[180,80,150,170,40,70, 110,30, 40,10,90,120,60]	
	Total Toll	0	730	
	Average Toll	0	146	
	Flow Vectors S2	[0,1,0,0,0,1,0,0,1,0,0,0,0]	[0,1,0,0,0,1,0,0,1,0,0,0,0]	
	Flow Vectors S3	[0,0,1,0,0,1,0,0,1,0,0,0,0]	[0,0,0,0,1,0,0,0,1,0,0,0,0]	
	Travel Time (h)	1111	1136	2.26
Carrier 2 Hazmat 1	Toll Vectors	-	[50,150,190,70,40,20, 0,0,60,140, 20,10,160]	
	Total Toll	0	2160	
	Average Toll	0	240	
	Flow Vectors S4	[0,0,1,0,0,1,0,0,1,0,1,0,1]	[0,0,0,0,1,0,0,0,1,0,1,0,1]	
	Flow Vectors S5	[0,0,0,0,0,1,0,0,1,0,1,0,0]	[0,0,0,0,0,1,0,0,1,0,1,0,0]	
	Travel Time (h)	2245	2289	1.93
Carrier 2 Hazmat 2	Toll Vectors	-	[180,80,150,170,40,70, 110,30,40,10,90,120,60]	
	Total Toll	0	10	
	Average Toll	0	10	
	Flow Vectors S6	[0,0,0,0,0,0,0,0,1,0,1,0,0]	[0,0,0,0,0,0,0,0,0,0,1,0,0,0]	
	Travel Time (h)	65.38	67.92	3.88
Risk	Maximum Arc Risk	2,499,955	1,085,507	-56.58
	Total Risk	4,766,543	3,682,296	-22.75

Travel time (total for the network) are in hours. See caption to Figure A-1 in Appendix, for explanation of the flow-vector notation.

5.2 Trade-off analysis

For the purpose of this trade-off analysis, we do not consider the toll cost term in the upper level model because it may overly influence our results. In the upper level, we have a two-objective problem. Hence a weighted sum method is employed to transform the two objectives into a single objective. The importance of one objective over another can be represented by applying a larger coefficient. In this section, 11 tests with different coefficients are run to see whether the improvement in total risk (risk equity) will have the opposite effect on risk equity (risk). The weights 1 and 2 in the second and third columns are coefficients of total risk and risk equity, respectively. For us, both coefficients are 0.5 in the base case.

Table 5.4: Trade-offs between the Total Risk and Risk Equity

Case No.	Weight 1	Weight 2	Total Risk(000)	Risk Equity(000)
T1	0	1	9,888	1,864
T2	0.1	0.9	9,210	2,006
T3	0.2	0.8	8,982	2,097
T4	0.3	0.7	8,723	2,145
T5	0.4	0.6	8,589	2,188
T6	0.5	0.5	8,462	2,218
T7	0.6	0.4	8,333	2,238
T8	0.7	0.3	8,193	2,302
T9	0.8	0.9	7,901	2,435
T10	0.9	0.1	7,760	2,518
T11	1	0	7,533	2,895

Our trade-off experiments are based on Case 8-4, with 27 regular demands and 15 hazmat demands. Results of the trade-offs between the total risk and risk equity are given in Table 5.4. A scatter diagram (Figure 5.1) is also drawn to show the relationship between these attributes. Both “Total Risk" and “Risk Equity" are mentioned as the

number of people exposed to a hazmat incident. Thus, a smaller value is preferable for each.

As we can see, Case T1 has the minimum risk equity, while Case T11 has the smallest total risk. These are the two extreme cases in our experiments. When comparing T1 with T6 (base case), the risk equity improves by 20 %, whereas total risk increases by 17 %. The enhancement in risk equity is primarily due to forcing carriers to use roads which are not used by others, in order to spread the risk. On the other hand, the min-total-risk case obtains solutions with smallest total risk because carriers choose less risky roads, regardless of risk equity.

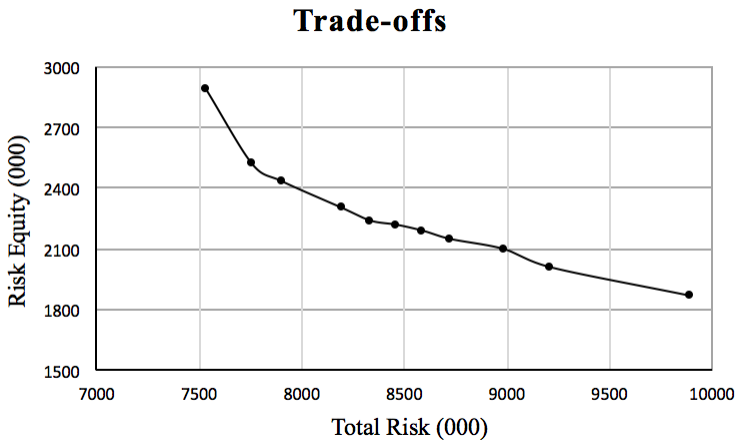

Figure 5.1: Trade-offs between Total Risk and Risk equity

From Figure 5.1, it is clear that with decreasing total risk, the risk equity is increasing. Hence, the improved total risk can be achieved at the expense of worsening risk equity. In addition, from T1 to T10, total risk changes more rapidly than risk equity. As a result, in these cases, total risk dominates risk equity. However, in going from T10 to T11, the increase in risk equity is larger than the decrease in total risk.

From Table 5.4, we see that T1 has a total risk of 9.89 million and risk equity of 1.76

million, whereas T11 has the lowest total risk but an extremely unfavourable value of risk equity. Since each of these is associated with a different safety issue during the transportation process, in our case, we consider both total equity and risk equity. Besides, results for the weights of Cases T5 and T7 are very similar to the results of T6. Therefore, it is appropriate for us to give these two kinds of risk an equal coefficient, which is 0.5, like Case T6 in our problem.

5.3 Variation of the Maximum Toll Value

To investigate the effect of the maximum toll cost, which was set at $200 in our base case, two additional settings are considered: maximum toll of $100, and maximum toll of $400. The detailed comparison of these three cases is provided in Table 5.5. Note that these results are the *average* of ten experiments based on Case 8-3. Both regular and hazmat travel times are measured in hours.

Table 5.5: Impact of Maximum Toll Value

Max Toll ($)	100	200	400
Total Risk (000)	3,862	3,769	3,645
Maximum Link Risk (000)	1,147	1,037	1,000
Regular Travel Time (000)	708	711	710
Hazmat Travel Time (000)	4.6	4.5	4.3
Regular Cost (000)	14,479	14,918	15,724
Hazmat Cost (000)	110	112	113
Avg. Regular Toll	106	205	420
Avg. Hazmat Toll	110	254	422

Both regular and hazmat cost refer to the total transportation cost, including toll cost.

As the value of the maximum toll increases, both total risk and risk equity have been

improved. Comparing the cases (Max Toll $200 and Max Toll $400), total risk is reduced in the latter by 3.3%; at the same time, risk equity of that case is enhanced by 3.6%. The main reason behind this phenomenon is that, when the maximum toll increases, it has more power to direct both the regular and hazmat carriers into less risky routes. Thus, the enhancement in total risk and risk equity can be achieved at the expense of a higher maximum toll.

The increases in both regular and hazmat cost are largely due to the average toll cost. The changes in regular and hazmat travel times are rather small. Therefore, the maximum toll value does not have a great influence on these two kinds of travel time. In addition, we also did experiments when the maximum toll is set to $800. However, the total risk and risk equity did not improve any more. Hence, when the maximum toll is below a certain value, the total risk and risk equity have positive relationships to the toll. However, when the maximum toll is above this value, it may not improve the risk.

5.4 Partition Scheme and PL-FW Comparisons

Table 5.6 summarizes linearization results,with different partition schemes, for the lower-level problem in our model. These are based on Cases 8-3, 15-4 and 24-7. Note that entries in the second column (partition scheme) denote the number of segments into which the feasible domain of v_a (i.e., $[0, \bar{v_a}]$) has been partitioned. The run times in the fifth and seventh columns are the $average$ times of the 10 experiments we did for each situation; values of the lower level objective function are written in thousands. The case with computational time > 7200 implies that the optimality gap does not reach zero within two hours, hence the data recorded corresponds to the case of 2 hours.The last column, % Difference between PL and FW, is calculated by (FW Results - PL Results)/ PL

Results ×100%.

Table 5.6: Results for Piecewise Linearization Approach under Different Partition Schemes

Case No.	Partition Scheme (# intervals)	PL Results	Opt. Gap (%)	Run Time(s)	FW Results	Run Time(s)	% Difference between PL and FW
8-3	20	2,841	0	10	2,755	1	-2.82
	50	2,801	0	21			-1.62
	100	2,750	0	86			0.21
	200	2,738	0	1,913			0.58
15-4	50	6,222	0	6,509	6,042	5	-2.89
	100	6,074	45	>7,200			-0.52
	150	6,053	77	>7,200			-0.12
	200	6,015	96	>7,200			0.44
24-7	5	-	100	>7,200	1,754	148	-
	10						
	20						
	40						

In this table, the total demand for 8-node, 15-node and 24-node networks is 3450, 4115 and 376.53, respectively. Therefore, the FW result of 24-node case is much smaller than for the case of 8 nodes or 15 nodes. Detailed information on the demand matrix is provided in Appendix A.

It is easy to conclude that a finer scheme, which partitions the feasible region into a greater number of smaller zones, requires longer computation time, but generates better solutions. For example, in Case 8.3, when the partition scheme increases from 100 to 200 sub-intervals, the lower-level objective decreases from 2.75 billion to 2.74 billion, a reduction of 0.37%. However, the computation time changes from 86 seconds to 1913 seconds, i.e. 21 times as long as before. Therefore, to find an appropriate partition scheme, it is important for us to trade off between better values of objective functions and computational time.

In addition, the size of the network and the demands of regular drivers also have

an effect on the computation time of the linearization approach. Comparing Case 8-1 (6 regular demands, 2 hazmat demands) to Case 8-3 (27 regular demands, 6 hazmat demands) when the number of intervals is 200, the computational time of the former is 972s, versus 1913s for the latter. This is because in Case 8-3, the greater demands can make the network a little more complicated. We also compare Case 8-3 with Case 15-3 (27 regular demands, 6 hazmat demands) when the feasible region is divided into 100 intervals. Although both cases have the same regular and hazmat demands, the running time for the latter (4005s) is nearly 50 times as large as the former (86s). The network of Case 15-3 is more complicated than that of Case 8-3, making the computational time longer.

Notice that, in all cases, the piecewise linearization approach can quickly develop "quality solutions" [same values as what we show in the third column (PL Results) of Table 5.6], but then this approach may require much more time to decrease the optimality gap. For instance, in Case 8-3, when the partition scheme involves 200 intervals, we reach the reported PL result (2,738) in 945 sec, with an optimality gap of 35%. Afterwards, the incumbent solution stays the same, but the optimality gap continues to decrease. Then, after almost another 1000 sec of computation time, the PW still shows the same solution but with 0 optimality gap. The reason behind this is that, although the solutions do not change, the best lower bound improves. Thus, the optimality gap greatly decreases. Another interesting finding is that when the feasible region is divided into more segments, within the same run time, the optimality gap becomes larger. For example, in Case 15-4, the optimality gaps for 100, 150 and 200 intervals are 45, 77 and 96%, respectively, when the computation time is restricted to 2 hours.

With the same partition scheme, and lower bound and upper bound, the running time can vary for each test because of a different initial solution. Consider Case 8-3 as an

example. When the partition scheme contains 100 intervals, the run times are between 71.55 and 108.42 sec. The reason is that the piecewise linearization approach chooses the initial solution $randomly$. Hence, the test whose starting solution turns out to be better can reach optimality in a shorter time.

Moreover, in Table 5.6, when we compare the two methods, we find that the computation time has been greatly improved by the Frank-Wolfe algorithm. For example, in Case 15-4, even when the number of intervals is only 50, the piecewise-linear computation time is 6,509 sec. However, the Frank-Wolfe algorithm takes only 5 sec to attain its results. As for the 24-node example, we cannot find an optimal solution with the piecewise linearization approach because of the huge computational requirements. However, the difference in results between these two methods is within 3% in Table 5.6.

Thus, the Frank-Wolfe algorithm is good enough to reasonably approximate the global optimum for this problem. In conclusion, the piecewise linearization approach is used for the 8-node and 15-node networks because of its accuracy and acceptable computation time. However, for the 24-node network, considering its complexity, we chose to use the Frank-Wolfe algorithm.

5.5 Convergence Analysis

A genetic algorithm is a multiple-direction searching method. It selects the best population, then applies the crossover and mutation operators within this population. Finally, it produces a new generation in each iteration. When the results do not improve for a certain number of generations, implying convergence, one halts the genetic algorithm. Ten tests are done in each subsection to see the effect on convergence speed of the crossover, mutation rate, population size and the number of generations. The mean number of

generations required for convergence and the objective function values will be recorded. During the first two subsections, the population size and number of generations are both constant at 40.

5.5.1 Crossover Rate

In this test, three values of the crossover rate are chosen: 0.7, 0.8 and 0.9. The mutation rate stays at 0.03 for all experiments. Detailed experimental results with these crossover rates are shown in Table 5.7.

Table 5.7: Results of GA Performance under Different Crossover Rates

Crossover Rate	0.7	0.8	0.9
# of Generations for Convergence	7	8	27
Obj. Function Value	14,443	13,433	13,172

The table indicates that the 0.7 crossover rate has the fastest speed, and 0.9 the slowest. However, results of the objective values are the opposite. 0.9 achieves the best, whereas 0.7 gets the worst objective function value. The reason this happens is that, when the crossover rate is a little lower, there is decreased chance explore the solution space. The result is therefore much more likely to be a local optimum. However, when the crossover rate is as high as 0.9, we can often find good results, but usually with too much computation time. Therefore, a crossover rate of 0.8 was chosen in our experiments because it gives us a good solution and enables a more rapid convergence.

5.5.2 Mutation Rate

In this subsection, three different mutation rates are chosen to explore their effect on convergence speed and performance of the genetic algorithm. Details are shown in Table

5.8.

Table 5.8: Results of GA Performance under Different Mutation Rates

Mutation Rate	0.01	0.03	0.05
# of Generations for Convergence	3	8	17
Obj. Function Value	13,945	13,433	12,412

The 0.05 mutation rate gets the best objective value but with the longest time. However, 0.01 has the fastest convergence speed, but its objective function value is not satisfactory. The reason behind this phenomenon is that, when the mutation rate is low, the solution set lacks diversity, and may be trapped in a local optimum. However, when the mutation rate is high, there is greater possibility of losing good solutions and more time is used. To minimize the possibility of losing good solutions, $elitist\ selection$ is applied after the mutation process. In elitist selection, we compare the new and the old solutions, and choose the better one. To trade off time and performance, a mutation rate of 0.03 has been used in our genetic algorithm solution.

5.5.3 Population Size

Population size also has great influence on the performance of the genetic algorithm. Normally, the larger the population size, the better results we will obtain. That is because a smaller population is going to lose diversity, and be trapped in a local optimum. In this subsection, we consider three population sizes, i.e. 20, 40 and 60. Details are summarized in Table 5.9.

In each experiment, the crossover rate and mutation rate remain at 0.8 and 0.03, respectively. In this table, as the population size grows from 20 to 60, the objective

Table 5.9: Results of GA Performance under Different Population Sizes

Population Size	20	40	60
# of Generations for Convergence	4	8	18
Obj. Function Value	15,083	13,433	11,441

function decreases from 15,083 to 11,441. This finding is consistent with our precious remarks on diversity. Although a population size of 60 gives the best solution to our model, we still need to trade off between convergence speed and objective function value. Therefore, a population size of 40 was chosen for our genetic algorithm calculations.

5.5.4 Number of Generations

The number of generation is an important stopping criterion in our genetic algorithm, affecting the performance. It is universally acknowledged that as the number of generations grows, results will improve. However, a great number of generations also means longer computing time. Therefore, it is important to trade off between that time and algorithm performance. The crossover and mutation rates stay at 0.8 and 0.03 during all the tests. The $average$ number of generations until convergence, and the objective function values, are given in Table 5.10.

Table 5.10: Results of GA Performance under Different Numbers of Generations

Numbers of Generation	20	40	60
# of Generations for Convergence	6	8	15
Obj. Function Value	14,668	13,434	12,887

Naturally, the largest number of generations, 60, achieves the best performance of the genetic algorithm. However, for 60 generations, nine out of ten experiments converged within the first 30 generations. Thus, to consider both convergence speed and performance, we chose 40 generations for our experiments in this chapter.

Chapter 6

Conclusions and Future Research

The dual toll pricing policy is a relatively new research area for hazmat transportation. Only a few researchers take regular traffic congestion into consideration when studying hazmat flows. In this thesis, a bi-level model based on a dual toll policy is developed. The upper level represents the government, attempting to minimize both the total risk and the maximum link risk. In addition, both upper level objective functions include the the total toll value, to ensure that the tolls set by the government are acceptable to each of regular traffic and hazmat carriers. The lower level problem represents the network users, including both regular and hazmat drivers; the priority concern for each of these groups is total transportation cost. In this bi-level model, the tolls are decided by the government. Once the tolls are given, both regular drivers and hazmat carriers can find their minimum cost path.

The bi-level model we applied in this thesis is a non-linear one; we know of no existing algorithm that can obtain a provably optimal solution to it. A solution method based on a genetic algorithm is proposed to deal with this model. Since the lower level consists of several non-linear terms, we first introduce a piecewise linearization to the lower level

in Section 4.2. Several findings are then developed in Chapter 5. First, the greater the number of segments, the longer the computation time required, but finer solutions can be obtained. Second, with a complicated network and heavy demands, the computational time increases. Third, the piecewise linearization approach can reach “quality solutions" quickly, but then additional time is used to diminish the gap between the incumbent solution and the best bound.

Considering of the long computation time of the piecewise linearization approach, we then introduced the Frank-Wolfe algorithm (Section 4.3) to solve our lower level problem. Although the Frank-Wolfe algorithm is not designed for a non-convex problem, we demonstrated its accuracy and efficiency for our problem.

The crossover rate, mutation rate and population size are three important parameters for a genetic algorithm. Therefore, to observe the relationship between these three parameters and convergence of the algorithm, an analysis is conducted in Section 5.4. From all these tests, we find that the rate of convergence has an important impact on the objective function values. Better solutions take more time. In our genetic algorithm, it is important for us to trade off between time and solution quality. Hence, we chose 0.8, 0.03, 40 to be our crossover rate, mutation rate and population size, respectively.

The fitness value is also an important part of a genetic algorithm, because the parents are selected based on their fitness to generate the children. In our model, the upper level objective functions are our fitness values. As we have seen, our upper level problem is a bi-objective model. Thus, a weighted sum method, with the coefficients of both functions set to 0.5, is used to find the fitness value. However, in an actual application, different coefficients can be used. A detailed study on the impact of these coefficients is presented in Section 5.2. We find that decreasing the risk equity increases the total risk. Hence, if authorities pay more attention to risk equity, a larger coefficient should be associated

with the risk equity term. By doing this, total risk is sacrificed for risk equity.

From the comparison of results before and after tolls (Table 5.2), it is easy to see that both total risk and maximum link risk are greatly improved, which is good news for the government.

To the best of our knowledge, very few papers combine a dual toll policy with several carriers and multiple hazmats. Moreover, we jointly consider the total risk, risk equity and transportation cost; other studies commonly consider only two of these three.

Several directions of research can be explored in the future. First, we found in Sec.5.4 that the random initial solution had a impact on the required computation time. Additional effort could be spent in the development of a heuristic to obtain a more consistent initial solution.

Second, although the genetic algorithm is an easy methodology to apply, it takes much calculation time. Therefore, different methods may be introduced to our model. One example is the modified Equilibrium-Decomposed Optimization heuristic proposed by Esfandeh et al. [2016]. They divided their whole problem into several subproblems corresponding to each arc, and then used a one-dimensional search routine to reduce approximate error.

Third, in our model, we assume all links can be tolled. However, due to technological restraints and traffic spill over, some links cannot be tolled. This kind of problem is normally referred to as 'second best'. [Johansson-Stenman and Sterner, 1998]. Such a problem has been addressed by Bard [2006]. With certain modifications, our model can also be extended to solve this 'second best' problem. For example, give these untolled arcs huge cost coefficients. A comparison between these two models can also be made.

Forth, as we saw, one major shortcoming of our policy is that for users in the network,

the benefits of the dual toll policy are unequal. For example, even carriers that have the same type of product may have unequal toll costs because different paths may have been chosen. Therefore, to improve the acceptability, $cost\ equity$ needs to be carefully defined and considered in future decision-making process.

Fifth, one of our major assumptions is that the flow of hazmat traffic is negligible when compared with regular flow. Although this assumption is true under most circumstances, there could be extreme situations where congestion can also be caused by hazmat carriers. This should be considered in the future.

Sixth, for hazmat carriers, we assume they cooperate with each other. However, in reality, the relationship between most carriers is competitive. Bianco et al. [2015] considered this aspect in their paper via a Nash equilibrium problem. In the future, maybe we can also use this method to analyse competition between carriers.

References

M. Abkowitz and P. D.-M. Cheng. Developing a risk/cost framework for routing truck movements of hazardous materials. *Accident Analysis & Prevention*, 20(1):39–51, 1988.

R. K. Ahuja and J. B. Orlin. Inverse optimization. *Operations Research*, 49(5):771–783, 2001.

V. Akgün, E. Erkut, and R. Batta. On finding dissimilar paths. *European Journal of Operational Research*, 121(2):232–246, 2000.

D. Aksen and N. Aras. A matheuristic for leader-follower games involving facility location-protection-interdiction decisions. In *Metaheuristics for Bi-level Optimization*, pages 115–151. Springer, 2013.

E. Alp. Risk-based transportation planning practice: Overall methodology and a case example. *INFOR: Information Systems and Operational Research*, 33(1):4–19, 1995.

J. M. Arroyo and F. J. Fernández. A genetic algorithm for power system vulnerability analysis under multiple contingencies. In *Metaheuristics for Bi-level Optimizatio*, pages 41–68. Springer, 2013.

G. Assadipour, G. Y. Ke, and M. Verma. A toll-based bi-level programming approach to managing hazardous materials shipments over an intermodal transportation network. *Transportation Research Part D: Transport and Environment*, 47:208–221, 2016.

J. Bard. Practical bilevel optimization: Algorithms and applications (nonconvex optimization and its applications). Secaucus, NJ, USA: Springer-Verlag, 2006.

R. Batta and S. S. Chiu. Optimal obnoxious paths on a network: transportation of hazardous materials. *Operations Research*, 36(1):84–92, 1988.

M. G. Bell. Mixed route strategies for the risk-averse shipment of hazardous materials. *Networks and Spatial Economics*, 6(3-4):253–265, 2006.

W. Bialas, M. H. Karwan, and J. Shaw. A parametric complementary pivot approach for two-level linear programming. *Operations Research Program Report, State University of New York at Buffalo*, 57(80-2), 1980.

L. Bianco, M. Caramia, and S. Giordani. A bilevel flow model for hazmat transportation network design. *Transportation Research Part C: Emerging Technologies*, 17(2):175–196, 2009.

L. Bianco, M. Caramia, S. Giordani, and V. Piccialli. Operations research models for global route planning in hazardous material transportation. In *Handbook of OR/MS Models in Hazardous Materials Transportation*, pages 49–101. 2013.

L. Bianco, M. Caramia, S. Giordani, and V. Piccialli. A game-theoretic approach for regulating hazmat transportation. *Transportation Science*, 50(2):424–438, 2015.

L. Brotcorne, M. Labbé, P. Marcotte, and G. Savard. A bilevel model for toll optimization on a multicommodity transportation network. *Transportation Science*, 35(4):345–358, 2001.

D. Burton and P. Toint. On the use of an inverse shortest paths algorithm for recovering linearly correlated costs. *Mathematical Programming*, 63(1-3):1–22, 1994.

D. Burton and P. L. Toint. On an instance of the inverse shortest paths problem. *Mathematical Programming*, 53(1-3):45–61, 1992.

W. Candler and R. Townsley. A linear two-level programming problem. *Computers & Operations Research*, 9(1):59–76, 1982.

P. Carotenuto, S. Giordani, and S. Ricciardelli. Finding minimum and equitable risk routes for hazmat shipments. *Computers & Operations Research*, 34(5):1304–1327, 2007a.

P. Carotenuto, S. Giordani, S. Ricciardelli, and S. Rismondo. A tabu search approach for scheduling hazmat shipments. *Computers & Operations Research*, 34(5):Computers & operations research, 2007b.

J. Current and S. Ratick. A model to assess risk, equity and efficiency in facility location and transportation of hazardous materials. *Location Science*, 3(3):187–201, 1995.

R. B. Dial. Minimal-revenue congestion pricing part i: A fast algorithm for the single-origin case. *Transportation Research Part B: Methodological*, 33(3):189–202, 1999.

E. Erkut and F. Gzara. Solving the hazmat transport network design problem. *Computers & Operations Research*, 35(7):2234–2247, 2008.

E. Erkut and A. Ingolfsson. Catastrophe avoidance models for hazardous materials route planning. *Transportation Science*, 34(2):165–179, 2000.

E. Erkut and A. Ingolfsson. Transport risk models for hazardous materials: revisited. *Operations Research Letters*, 33(1):81–89, 2005.

E. Erkut, S. A. Tjandra, and V. Verter. Hazardous materials transportation. *Handbooks in Operations Research and Management Science*, 14:539–621, 2007.

T. Esfandeh, C. Kwon, and R. Batta. Regulating hazardous materials transportation by dual toll pricing. *Transportation Research Part B: Methodological*, 83:20–35, 2016.

K. Fang, G. Y. Ke, and M. Verma. A routing and scheduling approach to rail transportation of hazardous materials with demand due dates. *European Journal of Operational Research*, 261(1):154–168, 2017.

M. Florian and D. Hearn. Network equilibrium models and algorithms. *Handbooks in Operations Research and Management Science*, 8:485–550, 1995.

M. Frank and P. Wolfe. An algorithm for quadratic programming. *Naval Research Logistics (NRL)*, 3(1-2):95–110, 1956.

M. Fukushima. A modified frank-wolfe algorithm for solving the traffic assignment problem. *Transportation Research Part B: Methodological*, 18(2):169–177, 1984.

R. Gopalan, K. S. Kolluri, R. Batta, and M. H. Karwan. Modeling equity of risk in the transportation of hazardous materials. *Operations Research*, 38(6):961–973, 1990.

A. Gupte, S. Ahmed, M. S. Cheon, and S. Dey. Solving mixed integer bilinear problems using milp formulations. *SIAM Journal on Optimization*, 23(2):721–744, 2013.

F. Gzara. A cutting plane approach for bilevel hazardous material transport network design. *Operations Research Letters*, 41(1):40–46, 2013.

P. Hansen, B. Jaumard, and G. Savard. New branch-and-bound rules for linear bilevel programming. *SIAM Journal on Scientific and Statistical Computing*, 13(5):1194–1217, 1992.

D. W. Hearn and M. V. Ramana. Solving congestion toll pricing models. In *Equilibrium and Advanced Transportation Modelling*, pages 109–124. Springer, 1998.

J. H. Holland. *Adaptation in natural and artificial systems: an introductory analysis with applications to biology, control, and artificial intelligence*. MIT press, 1992.

O. Johansson-Stenman and T. Sterner. What is the scope for environmental road pricing? *Road Pricing, Traffic Congestion and the Environment: Issues of Efficiency and Social Feasibility*, 1998.

Y. Kang, R. Batta, and C. Kwon. Generalized route planning model for hazardous material transportation with var and equity considerations. *Computers & Operations Research*, 43: 237–247, 2014.

B. Y. Kara and V. Verter. Designing a road network for hazardous materials transportation. *Transportation Science*, 38(2):188–196, 2004.

R. L. Keeney. Equity and public risk. *Operations research*, 28(3-part-i):527–534, 1980.

R. Klessig. An algorithm for nonlinear multicommodity flow problems. *Networks*, 4(4): 343–355, 1974.

M. Labbé, P. Marcotte, and G. Savard. A bilevel model of taxation and its application to optimal highway pricing. *Management Science*, 44(12-part-1):1608–1622, 1998.

T. Litman. Pricing for traffic safety: how efficient transport pricing can reduce roadway crash risks. *Transportation Research Record: Journal of the Transportation Research Board*, (2318):16–22, 2012.

P. Marcotte, A. Mercier, G. Savard, and V. Verter. Toll policies for mitigating hazardous materials transport risk. *Transportation Science*, 43(2):228–243, 2009.

Y. Marinakis and M. Marinaki. A bilevel particle swarm optimization algorithm for

supply chain management problems. In *Metaheuristics for Bi-level Optimization*, pages 69–93. Springer, 2013.

X. Meng, Q. Yunchao, and G. Ziyou. Implementing Frank-Wolfe algorithm under different flow update strategies and line search technologies. *Journal of Transportation Systems Engineering and Information Technology*, 8(3):14–22, 2008.

National Post. Lac mégantic train crash. `http://news.nationalpost.com/tag/lac-megantic-train-crash/`, 2013.

National Transportation Safety Board. Collision of cargo tank truck and automobile and subsequent fire. `https://www.ntsb.gov/investigations/AccidentReports/Pages/hazardous.aspx`, 2009.

J. Park, C. Kwon, and M. Son. Economic implications of the canada–us border bridges: Applying a binational local economic model for international freight movements. *Research in Transportation Business & Management*, 11:123–133, 2014.

C. ReVelle, J. Cohon, and D. Shobrys. Simultaneous siting and routing in the disposal of hazardous wastes. *Transportation Science*, 25(2):138–145, 1991.

N. Romero, L. K. Nozick, and N. Xu. Hazmat facility location and routing analysis with explicit consideration of equity using the gini coefficient. *Transportation Research Part E: Logistics and transportation review*, 89:165–181, 2016.

F. F. Saccomanno and A. Y. W. Chan. *Economic evaluation of routing strategies for hazardous road shipments*. Transportation Research Record, 1985.

R. A. Sivakumar, R. Batta, and M. H. Karwan. Establishing credible risk criteria for transporting extremely dangerous hazardous materials. *Transportation of Dangerous Goods: Assessing the Risks*, pages 335–342, 1993a.

R. A. Sivakumar, R. Batta, and M. H. Karwan. A network-based model for transporting extremely hazardous materials. *Operations Research Letters*, 13(2):85–93, 1993b.

R. A. Sivakumar, R. Batta, and M. H. Karwan. A multiple route conditional risk model for transporting hazardous materials. *INFOR: Information Systems and Operational Research*, 33(1):20–33, 1995.

C. Suwansirikul, T. L. Friesz, and R. L. Tobin. Equilibrium decomposed optimization: a heuristic for the continuous equilibrium network design problem. *Transportation Science*, 21(4):254–263, 1987.

UN. UN recommendation on the transport of dangerous goods, model regulations. united nations economic and social council's committee of experts on the transport of dangerous goods., 2001.

US DOT. Department of transportation federal railroad administration. `https://www.transit.dot.gov/regulations-and-guidance/safety/publications`, 1989.

US DOT. Hazmat summary by mode/cause: Calendar year 2003. `http://hazmat.dot.gov/pubs/inc/data/2003/2003scause.pdf`, 2004a.

US DOT. Hazmat summary by mode/cause: calendar year 2003. serious incidents, printed on january 4, 2005. the office of hazardous materials safety, us department of transportation, washington, dc, 2004b.

US DOT. Hazardous materials shipments by transportation mode. `https://www.rita.dot.gov/bts/sites/rita.dot.gov.bts/files/publications/`, 2012.

L. Vicente, G. Savard, and J. J. Júdice. Discrete linear bilevel programming problem. *Journal of Optimization Theory and Applications*, 89(3):597–614, 1996.

H. Von Stackelberg. *Marktform und gleichgewicht*. J. springer, 1934.

D. Z. Wang and H. K. Lo. Global optimum of the linearized network design problem with equilibrium flows. *Transportation Research Part B: Methodological*, 44(4):482–492, 2010.

J. Wang, Y. Kang, C. Kwon, and R. Batta. Dual toll pricing for hazardous materials transport with linear delay. *Networks and Spatial Economics*, 12(1):147–165, 2012.

Y. Wang and X. Qian. Stochastic block coordinate Frank-Wolfe algorithm for large-scale biological network alignment. *EURASIP Journal on Bioinformatics and Systems Biology*, 2016(1):9, 2016.

J. G. Wardrop and J. I. Whitehead. Correspondence. some theoretical aspects of road traffic research. *Proceedings of the Institution of Civil Engineers*, 1(5):767–768, 1952.

J. Y. Yen. Finding the k shortest loopless paths in a network. *Management Science*, 17(11): 712–716, 1971.

M. B. Yildirim and D. W. Hearn. A first best toll pricing framework for variable demand traffic assignment problems. *Transportation Research Part B: Methodological*, 39(8):659–678, 2005.

Appendix A

Appendix A provides further information about several examples we introduce in Chapter 5. Table A.1 includes the network topology and arc attributes for the 8-node network. Table A.2 develops the OD demand information for regular traffic, whereas shipments information about hazmat carriers are summarized in Table A.3. Similarly, the equivalent information about the 15-node network can be obtained from Tables A.4, A.5 and A.6. Tables A.7, A.8 and A.9 provide detailed information about the 24-node network. Figures A-1, A-2 and A-3 provide the network graphs for the cases of 8 nodes, 15 nodes and 24 nodes, separately.

Table A.1 Arc Attributes for the 8-node Network

Arc a		A_a	l_a	ρ_{a0} for hazmat 1	ρ_{a1} for hazmat 2
start	end				
1	2	6	900	701	1402
1	3	4	400	193	386
2	3	6	700	701	1402
2	4	5	200	1039	2078
2	5	4	100	193	386
3	5	4	250	800	1600
4	5	4	100	1295	2590
4	6	4	200	800	1600
5	6	2	300	1036	2072
5	7	6	250	1030	2060
6	7	2	150	1036	2072
6	8	4	350	1423	2846
7	8	5	100	1236	2472

Table A.2 Regular Travel Demand Matrix for 8-node Network

	1	2	3	4	5	6	7	8
1		70	50	50	90	290	300	300
2			100	80	40	100	70	300
3					10	25	150	400
4					150	120	200	50
5						100	90	80
6							120	60
7								50

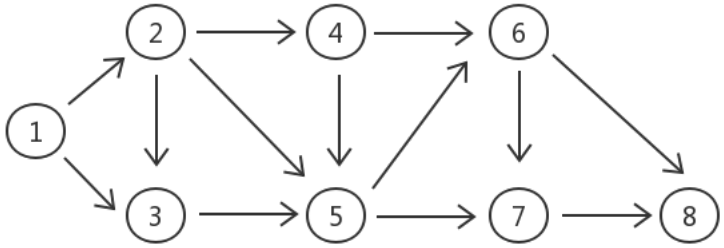

Figure A-1: 8-node network

Convention for Flow Vectors. See Table 5.3 (Regular, Before Toll): $(v_{12}, v_{13}, v_{23}, \cdots, v_{68}, v_{78})$ = (679, 741, 100, 780,419, 1011, 390, 780, 1080,720, 369,1031,209).

Table A.3 Hazmat Carriers Demand Matrix for 8-node Network

Hazmat Type	Hazmat 1			Hazmat 2		
Carrier Type	Carrier 1	Carrier 2		Carrier 1		Carrier 2
Shipment	S1	S2	S3	S4	S5	S6
O-D pair	1-4	1-6	2-6	2-8	3-7	5-7
ns	4	3	2	7	2	1

Table A.4 Arc Attributes for the 15-node Network

Arc a		A_a	l_a	ρ_{a0} for hazmat 1	ρ_{a1} for hazmat 2
start	end				
1	2	11	500	431	862
1	3	12	700	821	1642
2	3	3	300	808	1616
2	4	5	300	1171	2342
3	2	5	200	828	1656
3	4	4	400	778	1556
3	5	1	400	1278	2556
4	5	6	100	2196	4392
4	6	4	500	1004	2008
4	7	8	450	1255	2510
5	6	1	50	4576	9152
6	7	3	150	4576	9152
6	8	5	350	1074	2148
6	9	3	250	967	1934
6	11	10	800	1026	2052
7	8	1	600	4576	9152
8	9	3	450	1163	2326
9	10	5	200	492	984
9	11	7	350	978	1956
9	12	12	150	947	1894
10	12	5	250	205	410
10	13	2	100	890	1780
10	15	8	50	1082	2164
11	12	1	300	205	410
12	13	3	500	813	1626
13	14	5	300	85	170
14	15	1	250	85	170
15	14	3	300	957	1914

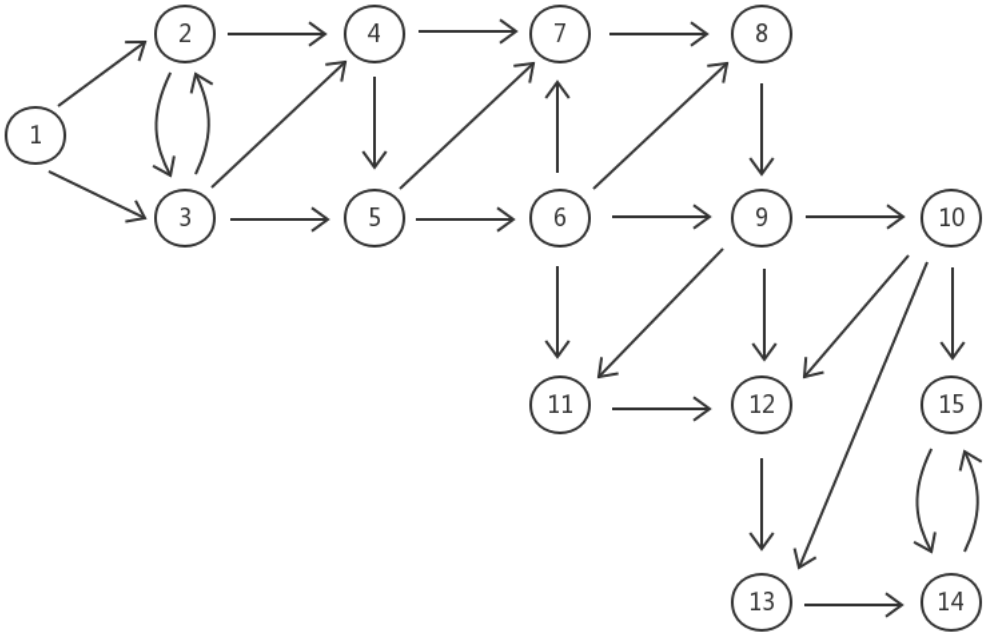

Figure A-2: 15-node network

Table A.5 Regular Travel Demand Matrix for 15-node Network

	1	2	3	4	5	6	7	8	9	10	11	12	13	14	15
1		100	40	20	10	140	110	90	80	170	50	20	120	300	300
2			60	50	100	90	40	150	120	60	20	100	300	250	240
3				50	50	60	80	400	100	200	45	35	50	30	100
4					85	40	10	60	50	100	30	10	300	60	100

Table A.6 Hazmat Carriers Demand Matrix for 15-node Network

Hazmat Type	Hazmat 1			Hazmat 2		
Carrier Type	Carrier 1	Carrier 2		Carrier 1		Carrier 2
Shipment	S1	S2	S3	S4	S5	S6
O-D pair	4-9	1-14	2-13	1-12	8-11	3-15
ns	3	3	7	7	2	4

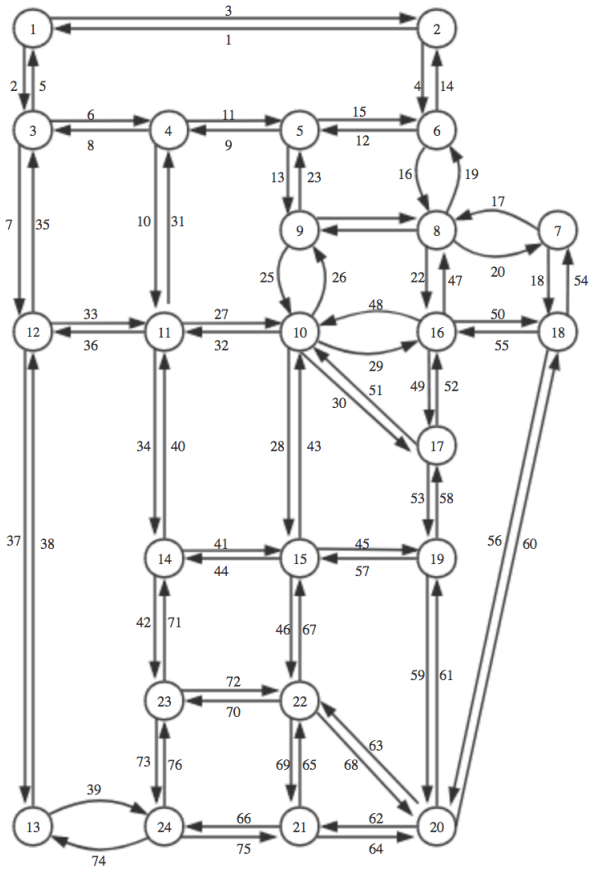

Figure A-3: 24-node network

Table A.7 Arc Attributes for the 24-node Network

Arc a		A_a	l_a	ρ_{a0} for hazmat 1	ρ_{a1} for hazmat 2	ρ_{a2} for hazmat 3
start	end					
1	2	0.06	25.90	6327	12654	9490.5
1	3	0.04	23.40	4218	8436	6327
2	1	0.06	25.90	6327	12654	9490.5
2	6	0.05	4.95	5273	10546	7909.5
3	1	0.04	23.40	4218	8436	6327
3	4	0.04	17.11	4218	8436	6327
3	12	0.04	23.40	4218	8436	6327
4	3	0.04	17.11	4218	8436	6327
4	5	0.02	17.78	2109	4218	3163.5
4	11	0.06	4.90	6327	12654	9490.5
5	4	0.02	17.78	2109	4218	3163.5
5	6	0.04	4.94	4218	8436	6327
5	9	0.05	10.00	5273	10546	7909.5
6	2	0.05	4.95	5273	10546	7909.5
6	5	0.04	4.94	4218	8436	6327
6	8	0.02	4.89	2109	4218	3163.5
7	17	0.03	7.84	3164	6328	4746
7	18	0.02	23.40	2109	4218	3163.5
8	6	0.02	4.89	2109	4218	3163.5
8	7	0.03	7.84	3164	6328	4746
8	9	0.1	5.05	10545	21090	15817.5
8	16	0.05	5.04	5273	10546	7909.5
9	5	0.05	10.00	5273	10546	7909.5
9	8	0.1	5.05	10545	21090	15817.5
9	10	0.03	13.91	3164	6328	4746
10	9	0.03	13.91	3164	6328	4746
10	11	0.05	10 .00	5273	10546	7909.5
10	15	0.06	13.51	6327	12654	9490.5
10	16	0.04	4.85	4218	8436	6327
10	17	0.08	4.99	8436	16872	12654
11	4	0.06	4.90	6327	12654	9490.5
11	10	0.05	10.00	5273	10546	7909.5
11	12	0.06	4.90	6327	12654	9490.5
11	14	0.04	4.87	4218	8436	6327

Table A.7 continued from previous page

Arc a		A_a	l_a	ρ_{a0} for hazmat 1	ρ_{a1} for hazmat 2	ρ_{a2} for hazmat 3
start	end					
12	3	0.04	23.40	4218	8436	6327
12	11	0.06	4.90	6327	12654	9490.5
12	13	0.03	25.90	3164	6328	4746
13	12	0.03	25.90	3164	6328	4746
13	24	0.04	5.09	4218	8436	6327
14	11	0.04	4.87	4218	8436	6327
14	15	0.05	5.12	5273	10546	7909.5
14	23	0.04	4.92	4218	8436	6327
15	10	0.06	13.51	6327	12654	9490.5
15	14	0.05	5.12	5274	10548	7911
15	19	0.03	14.56	3164	6328	4746
15	22	0.03	9.59	3164	6328	4746
16	8	0.05	5.04	5274	10548	7911
16	10	0.04	4.85	4218	8436	6327
16	17	0.02	5.22	2109	4218	3163.5
16	18	0.03	19.67	3164	6328	4746
17	10	0.08	4.99	8436	16872	12654
17	16	0.02	5.22	2109	4218	3163.5
17	19	0.02	4.82	2109	4218	3163.5
18	7	0.02	23.40	2109	4218	3163.5
18	16	0.03	19.67	3164	6328	4746
18	20	0.04	23.40	4218	8436	6327
19	15	0.03	14.56	3164	6328	4746
19	17	0.02	4.82	2109	4218	3163.5
19	20	0.04	5.00	4218	8436	6327
20	18	0.04	23.40	4218	8436	6327
20	19	0.04	5.00	4218	8436	6327
20	21	0.06	5.05	6327	12654	9490.5
20	22	0.05	5.07	5274	10548	7911
21	20	0.06	5.05	6327	12654	9490.5
21	22	0.02	5.22	2109	4218	3163.5
21	24	0.03	4.88	3164	6328	4746
22	15	0.03	9.59	3164	6328	4746
22	20	0.05	5.07	5274	10548	7911

Table A.7 continued from previous page

Arc a		A_a	l_a	ρ_{a0} for hazmat 1	ρ_{a1} for hazmat 2	ρ_{a2} for hazmat 3
start	end					
22	21	0.02	5.22	2109	4218	3163.5
22	23	0.04	5.00	4218	8436	6327
23	14	0.04	4.92	4218	8436	6327
23	22	0.04	5.00	4218	8436	6327
23	24	0.02	5.07	2109	4218	3163.5
24	13	0.04	5.09	4218	8436	6327
24	21	0.03	4.88	3164	6328	4746
24	23	0.02	5.07	2109	4218	3163.5

Table A.8 Regular Travel Demand Matrix for 24-node Network

	1	2	3	4	5	6	7	8	9	10	11	12	13	14	15	16	17	18	19	20	21	22	23	24
1	0	0.11	0.11	0.55	0.22	0.33	0.55	0.88	0.55	1.43	0.55	0.22	0.55	0.33	0.55	0.55	0.44	0.11	0.33	0.33	0.11	0.44	0.33	0.11
2	0.22	0	0.22	0.22	0.11	0.44	0.22	0.44	0.22	0.66	0.22	0.11	0.33	0.11	0.11	0.44	0.22	0	0.11	0.11	0	0.11	0	0
3	0.11	0.22	0	0.22	0.11	0.33	0.11	0.22	0.11	0.33	0.33	0.22	0.11	0.11	0.11	0.22	0.11	0	0	0	0	0.11	0.11	0
4	0.77	0.66	0.55	0	0.55	0.44	0.44	0.77	0.77	1.32	1.54	0.66	0.66	0.55	0.55	0.88	0.55	0.11	0.22	0.33	0.22	0.44	0.55	0.22
5	0.88	0.22	0.22	0.55	0	0	0.22	0.55	0.88	1.1	0.55	0.22	0.22	0.11	0.22	0.55	0.22	0	0.11	0.11	0.11	0.22	0.11	0
6	0.44	0.22	0.55	0.44	0.22	0	0.44	0.88	0.44	0.88	0.44	0.22	0.22	0.11	0.22	0.99	0.55	0.11	0.22	0.33	0.11	0.22	0.11	0.11
7	0.66	0.77	1.1	0.44	0.22	0.44	0	1.1	0.66	2.09	0.55	0.77	0.44	0.22	0.55	1.54	1.1	0.22	0.44	0.55	0.22	0.55	0.22	0.11
8	0.88	0.66	1.54	0.77	0.55	0.88	1.1	0	0.88	1.76	0.88	0.66	0.66	0.44	0.66	2.42	1.54	0.33	0.77	0.99	0.44	0.55	0.33	0.22
9	0.22	0.66	0.99	0.77	0.88	0.44	0.66	0.88	0	3.08	1.54	0.66	0.66	0.66	0.99	1.54	0.99	0.22	0.44	0.66	0.33	0.77	0.55	0.22
10	3.08	2.2	4.29	1.32	1.1	0.88	2.09	1.76	3.08	0	4.4	2.2	2.09	2.31	4.4	4.84	4.29	0.77	1.98	2.75	1.32	2.86	1.98	0.88
11	1.54	1.54	1.1	1.65	0.55	0.44	0.55	0.88	1.54	4.29	0	1.54	1.1	1.76	1.54	1.54	1.1	0.11	0.44	0.66	0.44	1.21	1.43	0.66
12	0.66	0.22	0.66	0.66	0.22	0.66	0.77	0.66	0.66	2.2	1.54	0	1.43	0.77	0.77	0.77	0.66	0.22	0.33	0.44	0.33	0.77	0.77	0.55
13	0.66	1.43	0.55	0.66	0.22	0.55	0.44	0.66	0.66	2.09	1.1	1.43	0	0.66	0.77	0.66	0.55	0.11	0.33	0.66	0.66	1.43	0.88	0.88
14	0.66	0.77	0.77	0.55	0.11	0.55	0.22	0.44	0.66	2.31	1.76	0.77	0.66	0	1.43	0.77	0.77	0.11	0.33	0.55	0.44	1.32	1.21	0.44
15	1.1	0.77	1.65	0.55	0.22	0.88	0.55	0.66	1.1	4.4	1.54	0.77	0.77	1.43	0	1.32	1.65	0.22	0.88	1.21	0.88	2.86	1.1	0.44
16	1.54	0.77	3.08	0.88	0.55	0.99	1.54	2.42	1.54	4.84	1.54	0.77	0.66	0.77	1.32	0	3.08	0.55	1.43	1.76	0.66	1.32	0.55	0.33
17	0.99	0.66	0	0.55	0.22	0.55	1.1	1.54	0.99	4.29	1.1	0.66	0.55	0.77	1.65	3.08	0	0.66	1.87	1.87	0.66	1.87	0.66	0.33
18	0.22	0.22	0.66	0.11	0	0.22	0.22	0.33	0.22	0.77	0.22	0.22	0.11	0.11	0.22	0.55	0.66	0	0.33	0.44	0.11	0.33	0.11	0
19	0.44	0.33	1.87	0.22	0.11	0.33	0.44	0.77	0.44	1.98	0.44	0.33	0.33	0.33	0.88	1.43	1.87	0.33	0	1.32	0.44	1.32	0.33	0.11
20	0.66	0.55	1.87	0.33	0.11	0.55	0.55	0.99	0.66	2.75	0.66	0.55	0.66	0.55	1.21	1.76	1.87	0.44	1.32	0	1.32	2.64	0.77	0.44
21	0.33	0.33	0.66	0.22	0.11	0.33	0.22	0.44	0.33	1.32	0.44	0.33	0.66	0.44	0.88	0.66	0.66	0.11	0.44	1.32	0	1.98	0.77	0.55
22	0.77	0.77	1.87	0.44	0.22	0.77	0.55	0.55	0.77	2.86	1.21	0.77	1.43	1.32	2.86	1.32	1.87	0.33	1.32	2.64	1.98	0	2.31	1.21
23	0.55	0.77	0.66	0.55	0.11	0.77	0	0.33	0.55	1.98	1.43	0.77	0.88	1.21	1.1	0.55	0.66	0.11	0.33	0.77	0.77	2.31	0	0.77
24	0.11	0.55	0.33	0.22	0	0.55	0	0	0	0.88	0.66	0.55	0.77	0.44	0.44	0.33	0.33	0	0.11	0.44	0.55	1.21	0.77	0

Table A.9 Hazmat Carriers Demand Matrix for 24-node Network

Hazmat Type	Carrier Type	Shipment	O-D pair	ns
Hazmat 1	Carrier 1	S1	10-11	0.02
		S2	10-12	0.03
		S3	11-17	0.01
	Carrier 2	S4	9-15	0.01
		S5	12-13	0.02
		S6	15-22	0.04
Hazmat 2	Carrier 1	S7	1-10	0.02
		S8	8-7	0.01
		S9	10-16	0.05
	Carrier 2	S10	11-14	0.03
		S11	17-20	0.03
		S12	22-16	0.05
Hazmat 3	Carrier 1	S13	8-16	0.02
		S14	10-19	0.01
		S15	15-17	0.02
		S16	16-17	0.03
	Carrier 2	S17	10-20	0.05
		S18	12-21	0.01
		S19	22-21	0.03
		S20	23-22	0.03